COORDINATION CHEMISTRY OF ARYLPHOSPHANES

Binding and interligand interactions in chromium, molybdenum and tungsten carbonyl complexes

LEENI HIRSIVAARA

Department of Chemistry,
University of Oulu

OULU 2001

LEENI HIRSIVAARA

COORDINATION CHEMISTRY OF ARYLPHOSPHANES

Binding and interligand interactions in chromium, molybdenum and tungsten carbonyl complexes

Academic Dissertation to be presented with the assent of the Faculty of Science, University of Oulu, for public discussion in Kajaaninsali (Auditorium L6), Linnanmaa, on June 16th, 2001, at 12 noon.

OULUN YLIOPISTO, OULU 2001

Manuscript received 7 May 2001
Manuscript accepted 14 May 2001

Communicated by
Professor Markku Leskelä
Professor Kari Rissanen

ISBN 951-42-5986-6 (URL: http://herkules.oulu.fi/isbn9514259866/)

ALSO AVAILABLE IN PRINTED FORMAT
ISBN 951-42-5985-8
ISSN 0355-3191 (URL: http://herkules.oulu.fi/issn03553191/)

OULU UNIVERSITY PRESS
OULU 2001

Hirsivaara, Leeni, Coordination chemistry of arylphosphanes
Department of Chemistry, University of Oulu, P.O.Box 3000, FIN-90014 University of Oulu, Finland
2001
Oulu, Finland
(Manuscript received 7 May 2001)

Abstract

The first part of this work consisted of a study of the coordination chemistry of aromatic (P,S) and (P,O) heterodonor phosphanes with $Cr(CO)_6$, $Mo(CO)_6$ and $W(CO)_6$. The (P,S) donor ligands having one or two *o* -thiomethoxyphenyl groups, preferred bidentate coordination mode, while the (P,O) donor ligands, having one, two or three *o* -methoxyphenyls, formed monodentate phosphorus bound complexes. Steric and electronic parameters affecting the coordination chemistry of the phosphanes are discussed for the monodentate complexes.

In the second part, triphenylphosphane and 2- and 4-pyridyldiphenylphosphane substituted tungsten tetracarbonyl derivatives was prepared, and attractive intramolecular interactions between the phosphane ligands were studied for both the neutral and the protonated complexes. Hydrogen bonding, π -stacking and cation-π bonding interactions were established, and observed to influence the *cis/trans* isomerism of the complexes. *Cis/trans* isomerism could be tuned by protonation, and deprotonation of the pyridyldiphenylphosphane derivatives.

All the complexes were characterised by ^{1}H, ^{13}C-{^{1}H} and ^{31}P-{^{1}H} NMR spectroscopy, X-ray crystallography, IR spectroscopy, and either elemental analysis or mass spectroscopy.

Keywords: cis/trans isomerism, NMR Spectroscopy, heterodonor phosphanes, intramolecular interactions

Acknowledgements

The present study was carried out in the Department of Chemistry at the University of Oulu, during the years 1998-2001.

I am most grateful to my supervisor Professor Jouni Pursiainen for his guidance, support and advice throughout the research. Furthermore, I am indebted to two referees, Professor Markku Leskelä and Professor Kari Rissanen, for their careful reading of the manuscript and Dr. Kathleen Ahonen for revising the language of my thesis.

I sincerely thank all my co-authors for their contributions. In particular, thanks are extended to Dos. Matti Haukka for his X-ray crystallographic work. I would also like to thank all my colleagues and the whole staff in the Department of Chemistry for a warm and supportive environment.

Warm thanks are owed to my husband Jani and my parents Eira and Antti for their invaluable encouragement during my work. The support of many friends has also been much appreciated.

The study was financed by the Inorganic Materials Chemistry Graduate Program and Neste Foundation. In addition, financial support from the Cultural Foundation of Pohjois-Pohjanmaa and Tauno Tönning Foundation is gratefully acknowledged.

Oulu, April 2001 Leeni Hirsivaara

List of original papers

This thesis is based on the following papers, which are referred to in the text by their Roman numerals:

I Hirsivaara L, Haukka M, Jääskeläinen S, Laitinen RH, Niskanen E, Pakkanen TA & Pursiainen J (1999) Organometallic derivatives of multidentate phosphines [o-(methythio)phenyl]diphenylphosphine and bis[o-(methylthio)phenyl]phenyl-phosphine. Preparation and characterization of group 6 metal carbonyl derivatives. J Organomet Chem 579: 45-52.

II Hirsivaara L, Guerricabeitia L, Haukka M, Suomalainen P, Laitinen RH, Pakkanen TA & Pursiainen J (2000) $M(CO)_6$ (M = Cr, Mo, W) Derivatives of o-(anisyl)diphenyl-phosphine, bis(o-anisyl)phenylphosphine, tris[o-anisyl)phosphine and (p-anisyl)bis(o-anisyl)phosphine, Inorg Chimica Acta 307: 47-56.

III Hirsivaara L, Haukka M & Pursiainen J (2000) Intramolecular hydrogen bonding and cation π-interactions affecting *cis-trans* isomerization in tungsten hexacarbonyl derivatives of 2-pyridyldiphenylphosphine and triphenylphosphane. Inorg Chem Comm 3: 508-510.

IV Hirsivaara L, Haukka M & Pursiainen J (2001) Intramolecular hydrogen bonding, cation-π and π-stacking interactions affecting *cis–trans* isomerization: tungsten hexacarbonyl derivatives of pyridyl substituted arylphosphane ligands. Eur J Inorg Chem, In press.

V Hirsivaara L, Haukka M & Pursiainen J (2001) Synthesis, crystal and molecular structure of a binuclear, double bridged hexacarbonyl tungsten derivative of 4-pyridyl-diphenylphosphane. J Organomet Chem, In press.

Symbols and abbreviations

Bu	butyl
HSQC	heteronuclear single-quantum correlation
L	ligand
Me	methyl
NMR	nuclear magnetic resonance
OMe	methoxy
o-OMePh	*ortho*-methoxyphenyl
Ph	phenyl
Py	pyridine
SMe	thiomethoxy
o-SMePh	*ortho*-thiomethoxyphenyl

Complexes synthesised in this work:

1 $[Cr(CO)_5(P(o\text{-}SMePh)Ph_2)]$
2 $[Cr(CO)_4(P(o\text{-}SMePh)Ph_2)]$
3 $[Mo(CO)_4(P(o\text{-}SMePh)Ph_2)]$
4 $[W(CO)_4(P(o\text{-}SMePh)Ph_2)]$
5 $[Cr(CO)_4(P(o\text{-}SMePh)_2Ph)]$
6 $[Mo(CO)_4(P(o\text{-}SMePh)_2Ph)]$
7 $[W(CO)_4(P(o\text{-}SMePh)_2Ph)]$

8 $[Cr(CO)_5(P(o\text{-}OMePh)Ph_2)]$
9 $[Mo(CO)_5(P(o\text{-}OMePh)Ph_2)]$
10 $[W(CO)_5(P(o\text{-}OMePh)Ph_2)]$
11 $[W(CO)_4(P(o\text{-}OMePh)Ph_2)_2]$
12 $[Cr(CO)_5(P(o\text{-}OMePh)_2Ph)]$
13 $[Mo(CO)_5(P(o\text{-}OMePh)_2Ph)]$
14 $[W(CO)_5(P(o\text{-}OMePh)_2Ph)]$
15 $[Cr(CO)_5\{P(o\text{-}OMePh)_3\}]$
16 $[Mo(CO)_5\{P(o\text{-}OMePh)_3\}]$
17 $[W(CO)_5\{P(o\text{-}OMePh)_3\}]$
18 $[Cr(CO)_5\{P(o\text{-}OMePh)_2(p\text{-}OMePh)\}]$

19 $[W(CO)_4(PPh_3)_2]$
20 $[W(CO)_4(PPh_3)(Py)]$

21 $[W(CO)_4(P(2\text{-}Py)Ph_2)_2]$
22 $[W(CO)_4(P(2\text{-}Py)Ph_2)(P(2\text{-}PyH)Ph_2)^+]ClO_4^-$
23 $[W(CO)_4(P(2\text{-}Py)Ph_2)(PPh_3)]$
24 $[W(CO)_4(P(2\text{-}PyH)Ph_2)^+(PPh_3)]ClO_4^-$

25 $[W(CO)_4(P(4\text{-}Py)Ph_2)]_2$

Contents

1 Introduction

Organophosphorus compounds were first synthesised in the early nineteenth century. Some 100 000 organophosphorus compounds were known by 1970, and many thousands more have been prepared since then. These compounds have been used for a variety of purposes: as agricultural chemicals, medicinal compounds, catalysts, flame retardants for fabrics and plastics, plasticising and stabilising agents in the plastics industry, selective extractants for metal salts from ores, additives for petroleum products and corrosion inhibitors [1].

Tertiary phosphanes, PR_3, are of special importance in organometallic chemistry and widely used in homogeneous catalysis. Examples of catalyst use include the Reppe compound used in alkene and acetylene polymerisation, the Wilkinson catalyst used in homogeneous hydrogenation of alkenes, and the tertiary phosphanes that enhance hydroformylation [1]. Water-soluble phosphanes in biphasic catalysis can be mentioned as an example of modern, environmentally benign phosphane chemistry [2].

Phosphanes are organic derivatives of PH_3, where the P(III) atom is tricoordinated [3]. In tertiary phosphanes all the hydrogen atoms are replaced by substituents, which variously may be aryl ring, alkyl chain, halogen atom or an electronegative group such as –OH or –SH. Parameters that describe the coordination behaviour of phosphane ligands describe either their steric properties or their electronic properties, including nucleophilicity [4] and basicity [5].

Steric properties that can be affected by size and shape of the substituents of the phosphane ligand are often described by cone angles, obtained either from X-ray structural data or by theoretical calculations [6,7]. Another measure of the steric requirements of a ligand is the ligand repulsive energy parameter E_R, which is based on a molecular mechanistic computational model [6]. The bulk of bidentate ligands can be evaluated by the bite angle (L-M-L) [8].

The basicity of the phosphanes can be described by pK_a values [9]: the greater the pK_a value, the more the ligand is considered to be susceptible to nucleophilic reactions. Usually, alkyl substituted phosphanes are more basic than arylphosphanes, and primary phosphanes are more basic than tertiary phosphanes [8]. pK_a values can be evaluated by

titrimetry [9,10]. Electron donor–acceptor properties of tertiary phosphane ligands have been estimated with the help of ν(CO) IR frequencies of $[Ni(CO)_3PR_3]$ [11].

Further parameters can be used to describe the electronic or steric character of the phosphanes in transition metal complexes: M-P bond lengths, spectroscopic parameters such as ^{31}P, ^{1}H and ^{13}C chemical shifts and coupling constants, infrared frequencies and intensities, electronic and magnetic dipole moments, and ionisation potentials of free ligands [12,13]. Ligand size can also have a marked influence on reaction rates and equilibria: dissociation of ligands, associative reactions, ligand exchange equilibrium, oxidative addition reactions and isomerism including *cis/trans* isomerism may all be affected by choice of ligand [13].

The variety of oxidation states for group 6 metals, ranging from –2 to +6, gives them a diverse coordination chemistry. The first row element chromium differs somewhat in its chemistry from molybdenum and tungsten. Group 6 hexacarbonyls, in which the metals are in oxidation state 0, are convenient starting materials for a variety of syntheses. Up to three carbonyl ligands of $M(CO)_6$ can be replaced by strong sigma donors (Lewis bases) such as tertiary phosphanes, isonitriles and amines [8]. A variety of phosphane derivatives, mostly monodentate, are known for $Cr(CO)_6$, $Mo(CO)_6$ and $W(CO)_6$ [14]. In this work, group 6 metals were chosen as a tool to study the coordination chemistry of tertiary phosphane ligands.

1.1 Heterodonor phosphanes

Synthesis of the multidentate phosphanes began with simple structures like $Ph_2PCH_2CH_2PPh_2$, and since then a considerable number of new and "tailor–made" phosphane ligands have been prepared [3]. The significance of the polyphosphanes has been increasing especially in the areas of homogeneous catalysis, asymmetric syntheses and organometallic stereochemistry, because the special properties of phosphanes can be accentuated by chelating [15]. Relative to monodentate phosphane ligands, polydentate phosphanes offer some advantages: increased nucleophilicity at the metal centre; more control over the coordination number, stoichiometry and stereochemistry of the resulting metal complexes; and slower and more controlled intra- and intermolecular exchange reactions [16]. The properties of multidentate phosphanes can be further modified by adding heterodonor atoms such as oxygen [17], nitrogen [18, 19] or sulphur [20].

Heterodonor ligands have become important in the development of the new homogeneous catalysts. The different properties of the donor atoms in functionalised phosphine ligands make the environment of the metal centre unsymmetrical and this may considerably alter the reactivity of the complex relative to the diphosphane derivatives. Furthermore, ligands that give rise to relatively weak chelate interactions offer the possibility for coordinative unsaturation without permanent ligand loss. Ether-type oxygen is a weakly chelating atom, which makes the transition metal complexes with phosphorus–oxygen donor ligands catalytically interesting: (P,O) donor ligands have tendency to form both a strong metal–phosphorus bond and one or more weak metal–oxygen bonds that can readily be cleaved in solution [17,21,22].

Heterodonor ligands are being studied in our laboratory, together with laboratories at the Helsinki University of Technology and the University of Joensuu, in a project targeting improved catalysts for hydroformylation. The results have been particularly promising in the hydroformylation of methyl methacrylate (MMA) with *in situ* prepared rhodium derivatives of heterodonor phosphanes. Ligands PPh_3, P(*o*-SMePh)Ph_2, P(*o*-OMePh)Ph_2, P(*o*-N(Me)$_2$Ph)Ph_2, $Ph_2PCH_2CH_2PPh_2$, $Ph_2P(CH_2)_4PPh_2$ and (*o*-SMePh)$_2PCH_2CH_2P$(*o*-SMePh)$_2$ have been found to have significantly different effects on conversions and the selectivities for products α- and β-methylformylisobutyrate (MFIB) [23]. The best overall result was obtained with ligand P(*o*-SMePh)Ph_2. This ligand was even more selective towards α-MFIB than are $Ph_2PCH_2CH_2PPh_2$ and $Ph_2P(CH_2)_4PPh_2$, which are highly selective in the α-hydroformylation of α,β-unsaturated esters. However, the reaction rate was lower than with PPh_3 [23].

Further studies with arylphosphane ligands having mixed sets of *o*-OMe, *o/p*-SMe, *o*-Me, pyridyl or naphtyl substituents [24,25] showed that all triarylphosphane ligands having one *o*-SMe substituent gave high α-selectivity in the hydroformylation of MMA regardless of the other substituent groups in the two phenyl rings. When the *ortho* substituent was unable to form chelate (*o*-Me, *o*-OMe), or the *o*-SMe was replaced with *p*-SMe, the selectivity changed significantly. Ligand P(*o*-OMePh)$_3$ gave no reaction, and P(*o*-SMePh)$_2$Ph gave only traces of products. Interestingly, ligand P(*o*-SMePh)(*o*-OMePh)$_2$ was highly selective. The chelation of the sulphur donor is regarded as the explanation for the high selectivity of mono *o*-SMe substituted ligands [25,26]. The effect of process variables on the regioselectivity has also been investigated [27].

Related ligands have been studied in the hydroformylation of 1-hexene and propene [28]. In 1-hexene hydroformylation, fairly high isomerisation activity was associated with all ligands studied. The main product was 2-hexene, and no hydrogenation was detected. In propene hydroformylation, the activity was highly dependent on the modification of the ligand, P(*o*-N(Me)$_2$Ph)Ph_2 being the only heterodonor ligand to give a proper reaction. The effects of electronegativity and steric factors of the ligands on the hydroformylation were discussed.

In this work, the coordination chemistry of aromatic (P,S) and (P,O) heterodonor ligands was studied with group 6 metal carbonyls. The study includes two structurally analogous ligand series with *o*-thiomethoxy (*o*-SMe) and *o*-methoxy (*o*-OMe) substituted triarylphosphanes. All (P,S) and (P,O) heterodonor ligands included in this study are covered with a patent for the hydroformylation of olefinic compounds [29]. The thiomethoxyphenyl substituted ligands formed mainly bidentate (P,S) chelates of the type $[M(CO)_4L]$ with group 6 metal carbonyls, while the methoxyphenyl substituted ligands formed monodentate, phosphorus bound complexes of the type $[M(CO)_5L]$. Chapter 2 describes the syntheses of the ligands and complexes, and chapter 3 presents the results and discussion.

1.2 Supramolecular organometallics

Supramolecular chemistry is one of the fastest growing areas of experimental chemistry. It can be defined as the chemistry of molecular assemblies and of intermolecular bonding, chemistry beyond the molecule, chemistry of the noncovalent bond or "nonmolecular chemistry". Specific applications are molecular recognition, catalysis and transport [30]. Supramolecular interactions can be classified as ion–ion interactions, ion–dipole interactions, dipole–dipole interactions, hydrogen bonding, cation-π interactions, π-stacking, Van der Waals forces, close packing in the solid state and hydrophobic effects [30].

Supramolecular organometallic chemistry covers the interactions both between metal and ligand and between ligands. Metal–to–ligand interactions are studied in the following areas: supramolecular self-assembly by dative bonding between metal and ligand, self-assembly by formation of secondary bond between the metal and the ligand, ionic interactions between electropositive metal and ligand and π-bonding between metal and ligand [31]. The ligand to ligand interactions that have been most extensively studied are self-assembly by hydrogen bond interactions and second sphere coordination [31,32]. Pyridine based ligands are common in the transition metal complexes used in molecular recognition and host-guest chemistry [33, 34].

In organometallic chemistry, the repulsive interactions together with electronic effects are important parameters in determining the structures and reactivity of complexes [13,35,36,37]. In contrast, the attractive interactions between ligands in the coordination sphere of a single transition metal complex have attracted much less attention as a means of understanding the associated structural and chemical phenomena. Studies have nevertheless been made in intramolecular π-stacking in transition metal complexes, both interligand and intraligand [38,39,40,41,42]. For example, arene π-stacking has been used as an intramolecular brake to prevent ligand rotation [43]. As well, studies have been done in interligand hydrogen bonding in biochemically interesting purine and pyrimidine complexes [44,45], and theoretical studies have been made of interligand hydrogen bonding between nitrogen donor ligands and small ligands such as H_2O, HF and NH_3 [46,47]. Further, there are a couple of reports on interligand CH-π interactions [48,49]. In fact, the interactions playing a vital role in enzyme catalysis at the active site of an enzyme–substrate complex in a metalloenzyme have been interpreted as ligand–ligand interactions around the metal atom [48].

The full potential of the above mentioned attractive interactions between ligands has not yet been evaluated: there are, for example, interests in synthesising catalyst molecules with rigid *cis* stereochemistry [50], and in addition to chelating ligands [51] attractive interactions could offer a route to overcome the steric repulsion. In catalytic reactions, specific, tailored attractive interactions between ligand and incoming substrate could increase the selectivity of the catalyst enormously. The attractive interactions between ligands or between ligand and substrate indeed suggest a very promising approach to organometallic catalysis.

In this work, attractive interactions between phosphane ligands were used to influence the *cis/trans* isomerisation in complexes of the type $[W(CO)_4L_2]$. The stereochemically almost identical ligands PPh_3, $P(2\text{-}Py)Ph_2$ and $P(4\text{-}Py)Ph_2$ were included in the study.

Pyridyl groups enhance the capability of ligands for attractive π-stacking, and pyridyl groups can be protonated with acid [52] to make interligand hydrogen bonding and cation-π bonding possible. Chapter 2 describes the syntheses of the ligands and complexes, and chapter 4 presents the results and discussion.

2 Experimental

The aim in the experimental part of this work was, first, to prepare group 6 metal carbonyl derivatives of a series of (P,O) and (P,S) heterodonor phosphanes and study their coordination chemistry and, second, to prepare pyridyldiphenylphosphane derivatives of tungsten hexacarbonyl, cabable of interligand supramolecular interactions. All the complexes were characterised by NMR spectroscopy, crystal structure analysis, IR spectroscopy and either elemental analysis or mass spectroscopy. If not commercially available, also the ligands were synthesised.

2.1 Reagents

Benzene and diethyl ether solvents were distilled from sodium/benzophenone ketyl under nitrogen before use. H_2O was saturated with nitrogen. Dichloromethane (Lab Scan), hexane (Lab Scan) and other solvents were used without further purification. $Cr(CO)_6$, $Mo(CO)_6$ and $W(CO)_6$ (Aldrich), $(CH_3)_3NO*2H_2O$ (Fluka Chemica), triphenylphosphane (Aldrich) and 2-pyridyldiphenylphosphane (Aldrich) were used as received. The other reagents were obtained from Aldrich, Merck or Fluka and used without further purification.

Analytical thin layer chromatography (TLC) was conducted on Kieselgel 60 F_{254} silica gel precoated aluminium plates (Merck). Column chromatography was carried out on silica gel.

2.2 Syntheses

All reactions were performed in inert atmosphere with standard Schlenk techniques. Ligand syntheses are described shortly in this section, even if the ligands were not new. Two routes were used in the preparation of the transition metal derivatives, one for the

derivatives of heterodonor ligands and the other for derivatives of pyridyldiphenyl-phosphanes.

2.2.1 Preparation of phosphane ligands

The phosphane ligands P(*o*-SMePh)Ph_2, P(*o*-SMePh)$_2$Ph, P(*o*-SMePh)$_3$, P(*o*-OMePh)Ph_2, P(*o*-OMePh)$_2$Ph, P(*o*-OMePh)$_3$ and P(*o*-OMePh)$_2$(*p*-OMePh) were synthesised by the method described in the literature [53,54]. 4-Pyridyldiphenylphosphane was prepared from 4-bromopyridine hydrochloride by a similar method at -100°C. The preparation reactions are shown in Scheme 1.

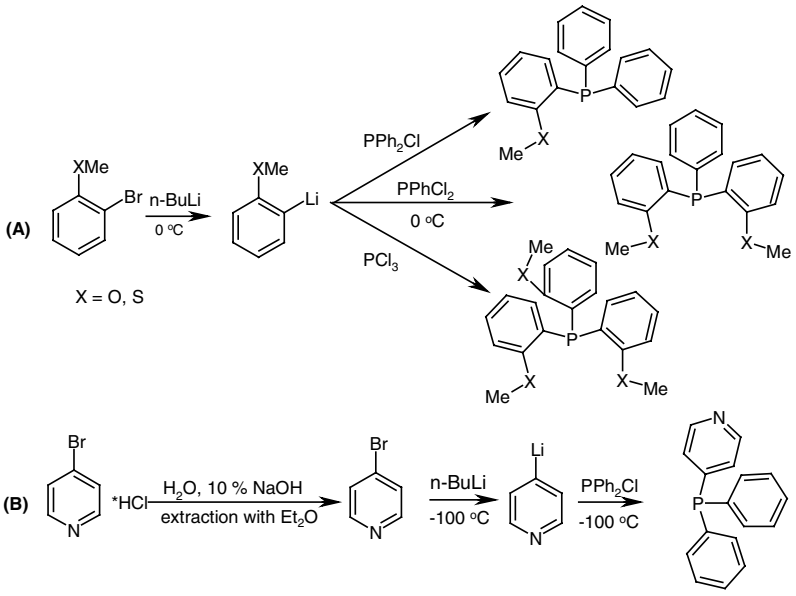

Scheme 1. Syntheses of heterodonor phosphanes (route A) and 4-pyridyldiphenylphosphane (route B).

2.2.2 Preparation of Cr, Mo and W carbonyl derivatives of (P,S) and (P,O) heterodonor phosphanes

The synthesis of Group 6 metal hexacarbonyl derivatives of heterodonor phosphanes was modified from the method described in the literature [55]. The metal hexacarbonyl, (P,S) or (P,O) heterodonor ligand and $(CH_3)_3NO*2H_2O$ were dissolved in dichloromethane,

and stirred for about 3 hours. The product was purified by column chromatography with use of dichloromethane–hexane mixtures as eluent. The single crystals were grown from dichloromethane–hexane mixtures by slow evaporation of the solvent.

2.2.3 Preparation of disubstituted tungsten carbonyl derivatives of triphenylphosphane and pyridyldiphenylphosphanes

The route for the synthesis of disubstituted tungsten tetracarbonyl complexes of pyridyldiphenylphosphanes was modified from the method described in the literature [56]. The starting material $[W(CO)_4(Py)_2]$ [57] was partly dissolved in benzene, the ligand (PPh_3, 2-$PyPh_2$ or 4-$PyPh_2$) was added and the mixture was stirred for 24 hours at 40°C. The product was purified by column chromatography using dichloromethane–hexane mixtures as eluent. Complex $[W(CO)_4(PPh_3)(P(2\text{-}Py)Ph_2)]$ was prepared by a similar method, from $[W(CO)_4(Py)(PPh_3)]$ as starting material. The crystals of the complexes were grown by slow evaporation of the solvent.

Protonation reactions of the complexes were carried out in $CDCl_3$ solution by adding perchloric acid diluted to about 26% water solution. Deprotonation reactions were carried out with 3 M CH_3COONa solution.

2.3 Instrumentation and measurements

NMR spectroscopy: The complexes were characterised with ^1H, ^{13}C-{^1H}, 2D HSQC and ^{31}P-{^1H} NMR spectra. Expect for some ^1H NMR spectra, the spectra were recorded on a Bruker DPX400 spectrometer, some of the ^1H NMR spectra were recorded on a Bruker AM200 spectrometer. ^1H, ^{13}C- and HSQC NMR spectra were referenced to internal tetramethylsilane (TMS) and ^{31}P NMR spectra to external 85% H_3PO_4. All samples were measured at room temperature with deuterated chloroform (99.8% D, 0.03% TMS, Aldrich).

^1H and ^{13}C-{^1H} NMR spectra of the complexes were interpreted on grounds of the spectra of free ligands, decoupling experiments and two–dimensional HSQC spectra. The assignments of the CO resonance peaks were based on the ^{13}C signal intensity ratios and the magnitude of the C-P coupling constants. In the ^{13}C-{^1H}NMR spectra of the free (P,S) and (P,O) donor ligands, the assignments of the aromatic carbons are based on calculated values [58] and the known spectra of triphenylphosphane. The C-P coupling constants support the interpretation. The ^1H NMR spectra of the ligands were interpreted with the help of decoupling experiments and HSQC spectra.

FTIR spectroscopy: FTIR spectra were recorded on a Bruker IFS 66 spectrometer, using dichloromethane as solvent. The spectra were measured at room temperature in a 0.1 mm KBr cuvette.

Mass spectroscopy: Exact masses were recorded with a Micromass LCT spectrometer using ESI+ method.

Elemental analyses: Elemental analyses were carried out on a Perkin Elmer 2400 Series II CHNS/O analyser.

X-ray crystallography: The X-ray measurements were performed at the University of Joensuu. Data were collected with a Nonius KappaCCD diffractometer at 20°C using Mo-Kα radiation (λ=0.71073 Å). Further details about the measurements are described in the original papers [I-V].

3 Cr, Mo and W carbonyl derivatives of (P, S) and (P, O) heterodonor phosphanes

Group 6 carbonyl complexes with phosphane ligands have been widely studied [14]. Several reports have also been published on bidentate (P, S) bound group 6 tetracarbonyl complexes, but there are only a few reports of arylphosphane derivatives containing a thioether–type sulphur atom in the chelate ring [20,59]. Monodentate complexes of the type $[Cr(CO)_5L]$ have been studied as a means of evaluating the steric and electronic properties of the phosphane ligands. Cone angles obtained from X-ray structural data or by mathematical modelling are important parameters for describing the steric restrictions of the ligands [6]. In addition, the electronic properties of the ligand have important effect

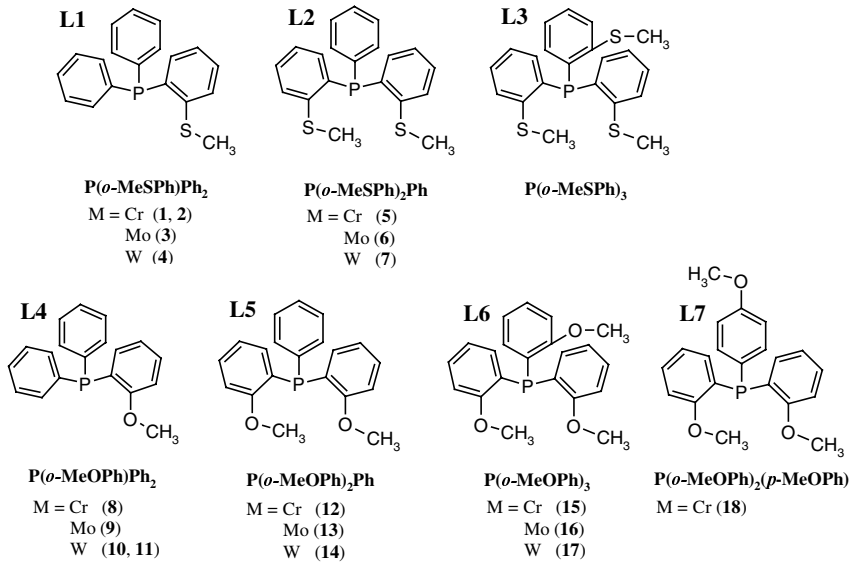

Scheme 2. Heterodonor ligands used in this work, and the transition metal derivatives prepared from the ligands.

on its coordination chemistry. ^{31}P NMR spectroscopy has been widely used in organometallic chemistry since the chemical shift is extremely sensitive to the electronic, steric and geometric environments of the ^{31}P nuclei [60].

In this work, study was made of the coordination chemistry of two structurally analogous arylphosphane series with *o*-OMe and *o*-SMe substituted phenyls (Scheme 2). The *ortho*-substituents make the ligands potentially multidentate, and they also affect the electronic and steric properties of the ligand.

The complexes were structurally characterised by multinuclear NMR and the structures of complexes were confirmed by single crystal X-ray diffraction study at the University of Joensuu.

3.1 Reactions

The reaction between metal carbonyl and the (P,S) donor ligands P(*o*-SMePh)Ph_2 and P(*o*-SMePh)$_2$Ph produced yellow, crystalline bidentate complexes of the type [M(CO)$_4$L]. In the reaction between P(*o*-SMePh)Ph_2 and Cr(CO)$_6$, some monodentate phosphorus bound complex [Cr(CO)$_5$(P(*o*-SMePh)Ph_2)] formed in addition to bidentate one, and refluxing was regimed to obtain only the bidentate complex. In the case of ligand P(*o*-SMePh)$_2$Ph too, the ^{1}H NMR spectrum showed signs of monodentate chromium carbonyl derivative, but only the bidentate complex could be isolated. The greater tendency of Mo and W to form bidentate compounds can be explained in terms of atomic radii [14] or kinetic effects.

No tridentate products could be obtained for the ligand P(*o*-SMePh)$_2$Ph. For example, an unsuccessful attempt was made to prepare tridentate product from complex [W(CO)$_4$(P(*o*-SMePh)$_2$Ph)] by refluxing it in THF for 3 h. Some attempts were made to prepare derivatives with potentially tetradentate ligand P(*o*-SMePh)$_3$, but no complexes could be isolated, even though some reaction seemed to occur.

The reaction between metal carbonyl and (P,O) donor ligands P(*o*-OMePh)Ph_2, P(*o*-OMePh)$_2$Ph, P(*o*-OMePh)$_3$ and P(*o*-OMePh)$_2$(*p*-OMePh) produced monodentate, phosphorus bound complexes of the type [M(CO)$_5$L]. In addition, tungsten hexacarbonyl showed some tendency to form a tetracarbonyl complex with two phosphane ligands in *cis* positions. No evidence of (P,O)-bound multidentate complexes was seen.

3.2 Structure and properties of complexes of (P,S) donor ligands

^{1}H NMR data of the (P,S) donor complexes (**1**-**7**) are presented in table 1 and the ^{13}C-{^{1}H} NMR data in table 2. Scheme 3 shows the numbering of the H and C atoms and the complexes. The ^{1}H signals for methyl protons were singlets, while the aromatic area was not of first order, and the signals were multiplets. In the ^{13}C-{^{1}H}NMR spectra, the signals were doublets (d) if the coupling constants are reported, and singlets (s) if not.

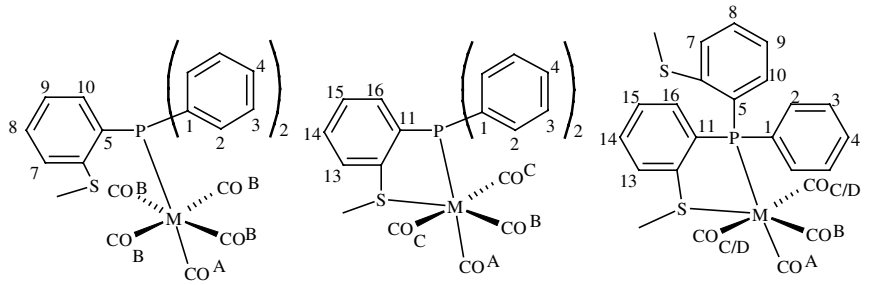

$[Cr(CO)_5(L1)]$ (**1**) $[M(CO)_4(L1)]$ M = Cr (**2**), Mo (**3**), W (**4**) $[M(CO)_4(L2)]$ M = Cr (**5**), Mo (**6**), W (**7**)

Scheme 3. Numbering of hydrogen and carbon atoms in NMR measurements.

*Table 1. ^{1}H chemical shifts (ppm) for (P,S) donor ligands (**L1, L2**) and complexes **1**-**7**. See scheme 3 for numbering of hydrogen atoms.*

	L1	**1**	**2**	**3**	**4**	**L2**	**5**	**6**	**7**
o-SCH_3	2.43	2.44	2.70	2.76	2.95	2.45	2.44	2.44	2.45
o-SCH_3	–	–	–	–	–	2.45	2.67	2.73	2.92
H(2,3,4)	7.32	6.95-7.70	7.35-7.48	7.35-7.45	7.32-7.45	7.30	7.18-7.79	7.19-7.70	7.28-7.78
H(7,8)	7.32	6.95-7.70	–	–	–	7.30	7.18-7.79	7.19-7.70	7.28-7.78
H(9)	7.04	6.95-	–	–	–	7.06	7.00	7.01	7.01
H(10)	6.76	7.70	–	–	–	6.74	6.17	6.28	6.25
H(13,14)	–	–	7.35-7.48	7.35-7.45	7.32-7.45	–	7.18-7.79	7.19-7.70	7.28-7.78
H(15)	–	–	7.53	7.51	7.51	–	7.18-7.79	7.19-7.70	7.28-7.78
H(16)	–	–	7.80	7.81	7.83	–	7.72	7.75	7.78

*Table 2. ^{13}C-{^{1}H} chemical shifts (ppm) and J_{CP} coupling constants (Hz) for (P,S) donor ligands (**L1**, **L2**) and complexes **1**-**7**. See scheme 3 for numbering of carbon atoms.*

	L1	**1**	**2**	**3**	**4**	**L2**	**5**	**6**	**7**
SCH_3	17.24	18.33	30.55	32.36	34.13	17.30	29.40	31.38	33.02
SCH_3	–	–	–	–	–	–	18.71	18.36	18.82
C(1)	136.25	134.99	135.94	136.51	135.71	135.46	137.07	136.94	136.90
$^{1}J_{CP}$	10 (d)	36 (d)	38 (d)	36 (d)	42 (d)	11 (d)	37 (d)	37 (d)	44 (d)
C(2)	134.01	133.44	132.06	132.30	132.29	134.32	133.27	133.41	133.46
$^{2}J_{CP}$	20 (d)	11 (d)	11 (d)	13 (d)	13 (d)	21 (d)	13 (d)	14 (d)	14 (d)
C(3)	128.57	128.58	128.69	128.63	128.66	128.64	129.00	128.92	129.15
$^{3}J_{CP}$	7 (d)	9 (d)	8 (d)	9 (d)	9 (d)	8 (d)	10 (d)	10 (d)	11 (d)
C(4)	128.82	128.62	128.72	128.92	128.99	128.93	129.05	129.17	129.42
C(5)	136.77	132.21	–	–	–	136.16	132.87	132.60	132.31
$^{1}J_{CP}$	10 (d)	36 (d)				10 (d)	40 (d)	38 (d)	43 (d)
C(6)	143.67	134.70	–	–	–	143.78	143.17	143.11	143.26
$^{2}J_{CP}$	27 (d)	36 (d)				29 (d)	14 (d)	14 (d)	12 (d)
C(7)	126.62	128.40	–	–	–	126.75	128.56	128.87	129.07
$^{3}J_{CP}$	(s)	(s)				4 (d)	(s)	(s)	(s)
C(8)	129.33	130.11	–	–	–	129.34	129.6-131.0	130.2-130.5	130.4-131.0
C(9)	125.35	125.36	–	–	–	125.34	125.35	125.16	125.20
$^{3}J_{CP}$	(s)	6 (d)					5 (d)	6 (d)	7 (d)
C(10)	133.91	132.14	–	–	–	133.35	129.6-131.0	130.2-130.5	130.4-131.0
$^{2}J_{CP}$	(s)	8 (d)							
C(11)	–	–	136.6	136.44	137.31	–	138.48	137.88	138.88
$^{1}J_{CP}$			34 (d)	33 (d)	38 (d)		31 (d)	32 (d)	37 (d)
C(12)	–	–	146.09	144.73	145.79	–	146.17	145.00	146.01
$^{2}J_{CP}$			36 (d)	33 (d)	31 (d)		36 (d)	31 (d)	30 (d)
C(13)	–	–	129.89	129.92	130.14	–	129.6-131.0	130.2-130.5	130.4-131.0
$^{3}J_{CP}$			(s)	(s)	(s)				
C(14)	–	–	133.70	134.30	134.46	–	132.67	133.96	134.07
C(15)	–	–	131.01	131.11	131.39	–	130.97	130.77	131.05
$^{3}J_{CP}$			(s)	(s)	(s)		(s)	(s)	(s)
C(16)	–	–	130.50	131.58	131.39	–	129.38	131.08	131.04
$^{2}J_{CP}$			10 (d)	10 (d)	10 (d)		6 (d)	8 (d)	8 (d)
C(A)	–	221.7	226.9	215.8	207.7	–	227.0	216.2	207.8
$^{2}J_{CP}$		(s)	(s)	27 (d)	30 (d)		(s)	30 (d)	30 (d)
C(B)	–	217.1	228.1	218.3	208.6	–	228.0	218.3	208.8
$^{2}J_{CP}$		13 (d)	11 (d)	8 (d)	6 (d)		11 (d)	6 (d)	6 (d)
C(C)	–	–	218.1	207.5	201.0	–	217.1	206.3	200.1
$^{2}J_{CP}$			11 (d)	8 (d)	6 (d)		12 (d)	6 (d)	(s)
C(D)	–	–	–	–	–	–	219.5	208.8	202.0
$^{2}J_{CP}$							15 (d)	8 (d)	6 (d)

When the bidentate complexes **2**-**7** were formed, the ^{1}H and ^{13}C chemical shifts of the SCH_3 group increased due to coordination of sulphur to the metal centre. This deshielding effect increased from Cr to Mo to W. In the case of monodentate derivative **1**, the resonance did not change markedly.

^{1}H and ^{13}C shielding of the phenyl rings did not change markedly upon coordination of the ligands. There were minor changes due to phosphorus coordination in the sulphur uncoordinated thiomethoxyphenyl rings of complexes **1** and **5**-**7**: shielding of the C(5) directly bonded to phosphorus increased by about 3.3-4.6 ppm, and there was slight increase in the shielding of C(10), and slight deshielding of (C7). The coordination of sulphur caused deshielding of the aromatic protons of thioanisole both in the ^{1}H and ^{13}C NMR spectra: the coordination of sulphur caused deshielding of the ^{13}C chemical shifts by 1-6 ppm compared with shifts of the free ligands. However, the chemical shift of C(11) in complexes **2**-**4** did not change, and the shift of C(16) was shielded a little in all (P,S) bound complexes. Change of the metal had no significant effect on the chemical shifts of the aromatic carbons.

For all the complexes, the coordination of phosphorus to the metal centre caused a clear increase in the $^{1}J_{CP}$ coupling constant. Actually, the $^{1}J_{CP}$ coupling changed from negative to positive because the phosphorus atom lost its nonbonding electron pair upon coordination to the metal centre [61]. The $^{2}J_{CP}$ coupling constants of thiomethoxyphenyls were dependent on sulphur coordination: the $^{2}J_{CP}$ coupling constants of the uncoordinated thiomethoxyphenyl rings and phenyls decreased due to the phosphorus coordination. In contrast to this, the $^{2}J_{CP}$ coupling constants of the sulphur coordinated thiomethoxyphenyl rings increased and no $^{3}J_{CP}$ coupling constants were observed.

The ^{13}C chemical shifts of carbonyl carbons decreased in the order Cr > Mo > W, in parallel with the increasing number of electrons in the metal [62]. The spectrum of monodentate phosphorus–bound complex **1** exhibited two carbonyl doublets due to the carbonyls oriented *trans* and *cis* to phosphorus. The spectra of the bidentate complexes **2**-**4** exhibited three doublets, indicating the presence of three types of carbonyls, one *trans* to phosphorus, one *trans* to sulphur and one *cis* to both phosphorus and sulphur. The carbonyl signals of the P(*o*-$SMePh)_2Ph$ substituted complexes **5**-**7** were in agreement with the crystal structures showing four non–equivalent doublets: one for carbonyl *trans* to P, one for carbonyl *trans* to metal bound S, one for carbonyl *cis* to both P and S, and one for carbonyl *cis* to both P and S but affected by a free SCH_3 group located near it.

$^{2}J_{CP}$ coupling constants of the carbonyl groups followed trends observed earlier: for chromium complexes $|^{2}J_{CP}(cis)| > |^{2}J_{CP}(trans)|$ and for molybdenum and tungsten complexes $|^{2}J_{CP}(cis)| < |^{2}J_{CP}(trans)|$ [62]. Coordination of sulphur had no apparent effect on the magnitude of the coupling constants.

The ^{31}P-$\{^{1}H\}$ NMR data of the complexes **1**-**7** is presented in table 3. The ^{31}P chemical shifts were clearly increased upon coordination of the ligand to the metal centre. The coordination shifts $\{\Delta\delta = \delta_P(\text{complex}) - \delta_P(\text{ligand})\}$decreased in the order Cr > Mo >W, in agreement with the observation that ^{31}P chemical shift should decrease as one descends in a given periodic group [63]. The ^{31}P chemical shift of the complex decreased with increasing number of *o*-thiomethoxy substituents in the ligand. Coordination shifts, on the other hand, increased with the number of *ortho* substituents.

*Table 3. ^{31}P-{^{1}H} chemical shifts (δ_p, ppm) and ^{31}P coordination shifts ($\Delta\delta$, ppm) for complexes **1**-**7** ($\Delta\delta = \delta_P(complex) - \delta_P(ligand)$).*

L	δ_P	Cr complex	δ_p	$\Delta\delta_P$	Mo complex	δ_p	$\Delta\delta_P$	W complex	δ_p	$\Delta\delta_P$
L1	-13	**1**	70	83	-			-		
L1	-13	**2**	84	97	**3**	62	75	**4**	51	64
L2	-22	**5**	78	100	**6**	55	77	**7**	46	68

The ^{31}P coordination shift difference between the monosubstituted P(*o*-SMePh)Ph_2 derivative of chromium (complex **1**) and its chelated analogue **2** was 14 ppm. The lower shielding of **2** can be explained in terms of chelate ring contributions. The typical ^{31}P deshielding in phosphorus–bound bidentate complexes relative to the corresponding monodentate structures is about 25-32 ppm [63]. It seems as if the deshielding effect of the phosphorus–sulphur chelate ring is weaker.

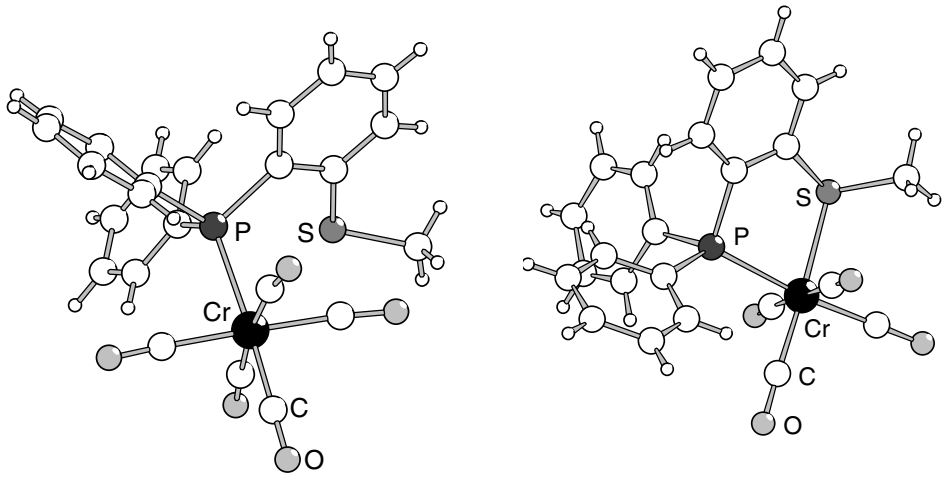

Fig. 1. Crystal structures of monodentate [$Cr(CO)_5$(P(*o*-SMePh)Ph_2)] (1) and its bidentate analogue [$Cr(CO)_4$(P(*o*-SMePh)Ph_2)] (2). Complexes [$Mo(CO)_4$(P(*o*-SMePh)Ph_2)] (3) and [$W(CO)_4$(P(*o*-SMePh)Ph_2)] (4) have a related structure than 2.

The crystal structures of all the complexes showed slightly distorted octahedral geometry. The structures were consistent with the NMR spectra, phosphane ligand having replaced two of the carbonyl ligands in each complex except the monodentate complex **1**. Figure 1 shows the crystal structures of the chromium carbonyl derivatives **1** and **2**. The Mo (**3**) and W (**4**) complexes of P(*o*-SMePh)Ph_2 had a similar bidentate structure to **2**. The structure of the molybdenum complex of potentially tridentate ligand P(*o*-SMePh)$_2$Ph is shown in Fig. 2. The P(*o*-SMePh)$_2$Ph derivatives with chromium and tungsten had a related structure.

Chromium hexacarbonyl derivatives had the shortest metal–to–ligand bond lengths, owing to the small atomic radius of chromium. Molybdenum derivatives tend to have slightly longer bonds around the metal centre than do the tungsten derivatives, as has been observed earlier [64]. In bidentate complexes, the M–S bond lengths were slightly longer than the M–P bond lengths. The M–P bond of the monodentate complex $[Cr(CO)_5(P(o\text{-}SMePh)Ph_2)]$ (**1**) was 2.431 Å, being longer than in the bidentate analogue $[Cr(CO)_4(P(o\text{-}SMePh)Ph_2)]$ (**2**) (M–P 2.354 Å, M–S 2.394 Å).

In all complexes (**1**-**7**), the M–C bond of the carbonyl *trans* to phosphorus was slightly shorter than the M-C bonds of the *cis*-carbonyls. Similarly, shortening of the M–C bond *trans* to sulphur was associated with sulphur coordination. Thus the M–C bond distances reflect the relative *trans* influence of the donors S < P < CO (ability of ligand L to weaken the M–L´ bond *trans* to it) [65].

Complexation caused some changes in the bond angles. In bidentate complexes (**2**-**7**), P–M–S angles were less than 90°, ranging from 77.5°(**3**) to 81.4° (**5**). The P–M–S angles in chromium derivatives were in average 81°, being about 3° wider than the average value in the molybdenum and tungsten derivatives. The P–M–S angle also induced deviations to the other angles, the carbonyl ligands being pushed away from the phosphane ligand.

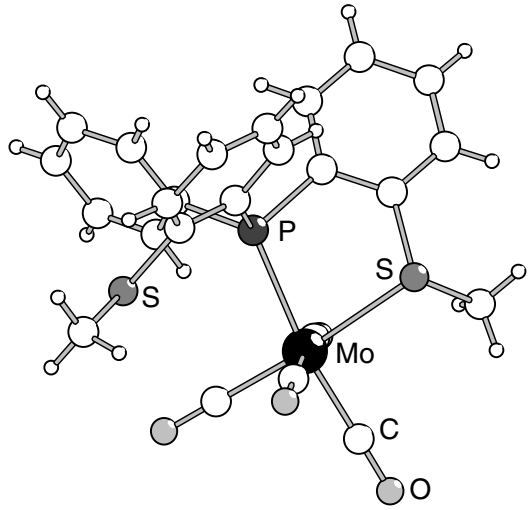

Fig. 2. Crystal structure of $[Mo(CO)_4(P(o\text{-}SMePh)_2Ph)]$ (6), in which one sulphur donor is coordinated and one is not. The corresponding chromium and tungsten complexes $[Cr(CO)_4(P(o\text{-}SMePh)_2Ph)]$ (5) and $[W(CO)_4(P(o\text{-}SMePh)_2Ph)]$ (7) have analogous structures.

3.3 Structure and properties of complexes of (P,O) donor ligands

^{1}H NMR data of the (P,O) donor complexes **8**-**10** and **12**-**18** are presented in table 4 and the ^{13}C-{^{1}H} NMR data in tables 5 and 6. Scheme 4 shows the numbering of the H and C

atoms in the complexes. The ^{1}H signals for the methyl protons were singlets, while the aromatic area was not of first order, and the signals were multiplets. In the ^{13}C-{^{1}H}NMR spectra, the signals were doublets (d) if the coupling constants are reported, and singlets (s) if not.

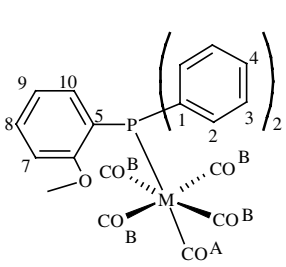

$[M(CO)_4(L4)]$
M = Cr (**8**), Mo (**9**), W (**10**)

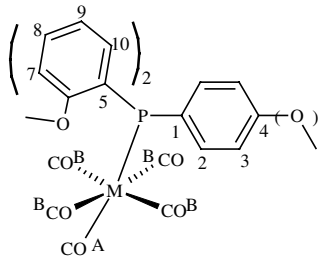

$[M(CO)_4(L5)]$
M = Cr (**12**), Mo (**13**), W (**14**)
$[Cr(CO)_4(L7)]$ (**18**)

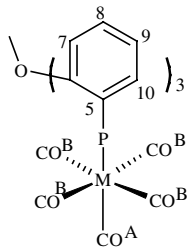

$[M(CO)_4(L6)]$
M = Cr (**15**), Mo (**16**), W (**17**)

Scheme 4. Numbering of hydrogen and carbon atoms in NMR measurements.

*Table 4. ^{1}H chemical shifts (ppm) for (P,O) donor ligands (**L4-L7**) and complexes **8-10, 12-18**. See scheme 4 for numbering of hydrogen atoms.*

	L4	**8**	**9**	**10**	**L5**	**12**	**13**	**14**
o-OCH_3	3.75	3.71	3.69	3.69	3.74	3.68	3.67	3.67
H(2)	7.25 -	7.36 -	7.37 -	7.38-	7.25-	7.58	7.56	7.56
H(3,4,8)	7.36	7.50	7.49	7.49	7.37	7.36- 7.45	7.36- 7.45	7.37- 7.45
H(7)	6.90	6.97	6.96	6.98	6.89	6.93	6.93	6.93
H(9)	6.86	6.95	6.93	6.95	6.85	6.91	6.90	6.92
H(10)	6.67	6.86	6.79	6.79	6.67	6.85	6.84	6.84
	L6	**15**	**16**	**17**	**L7**		**18**	
o-OCH_3	3.74	3.56	3.56	3.55	3.72		3.69	
p-OCH_3	–	–	–	–	3.80		3.83	
H(2)	–	–	–	–	7.22		7.50	
H(3)	–	–	–	–	6.80-6.90		6.86-6.92	
H(7)	6.88	6.87	6.87	6.87	6.80-6.90		6.92	
H(8)	7.33	7.38	7.40	7.39	7.31		7.41	
H(9)	6.84	6.95	6.95	6.96	6.80-6.90		6.86-6.92	
H(10)	6.67	7.36	7.31	7.32	6.68		6.82	

The ^{1}H and ^{13}C chemical shifts of the phosphanes correlated well with the shifts of the complexes. When the complexes were formed, the ^{1}H and ^{13}C shielding of the *o*-OCH_3 groups increased marginally. In contrast, the *p*-OCH_3 group of the complex **18** was

deshielded. This result might indicate some weak interaction between the oxygen atom or atoms in *ortho* positions and the metal centre [21].

As with the derivatives of the (P,S) donor ligands, the change of the metal did not have any significant effect on the chemical shifts of the aromatic carbons.

*Table 5. ^{13}C-{^1H} chemical shifts (ppm) and J_{CP} coupling constants (Hz) for (P,O) donor ligands (**L4**,**L5**) and complexes **8-10, 12-14**. See scheme 4 for numbering of carbon atoms.*

	L4	**8**	**9**	**10**	**L5**	**12**	**13**	**14**
OCH_3	55.66	54.53	54.57	54.66	55.66	54.45	54.54	54.64
C(1)	136.69	134.76	134.74	134.44	136.43	133.50	133.59	133.30
$^1J_{CP}$	10 (d)	38 (d)	37 (d)	43 (d)	10 (d)	37 (d)	36 (d)	42 (d)
C(2)	133.86	133.10	133.27	133.38	134.01	134.26	134.33	134.52
$^2J_{CP}$	21 (d)	11 (d)	13 (d)	12 (d)	21 (d)	12 (d)	14 (d)	13 (d)
C(3)	128.32	128.33	128.33	128.38	128.18	128.21	128.18	128.24
$^3J_{CP}$	7 (d)	10 (d)	10 (d)	10 (d)	8 (d)	10 (d)	10 (d)	10 (d)
C(4)	128.53	129.87	129.85	130.07	128.41	129.96	129.88	130.10
$^4J_{CP}$	(s)	2 (d)	2 (d)	2 (d)	(s)	2 (d)	2 (d)	2 (d)
C(5)	125.59	122.20	122.52	121.98	125.18	122.05	122.01	121.47
$^1J_{CP}$	11 (d)	36 (d)	35 (d)	41 (d)	13 (d)	37 (d)	35 (d)	42 (d)
C(6)	161.12	159.59	159.54	159.65	161.33	159.50	159.61	159.70
$^2J_{CP}$	16 (d)	6 (d)	7 (d)	6 (d)	16 (d)	7 (d)	7 (d)	6 (d)
C(7)	110.18	110.77	110.67	110.72	110.18	110.80	110.76	110.85
$^3J_{CP}$	(s)	4 (d)	4 (d)	4 (d)	(s)	4 (d)	4 (d)	4 (d)
C(8)	130.30	132.20	132.10	132.27	130.08	131.80	131.71	131.95
$^4J_{CP}$	(s)	1 (d)	(s)	1 (d)	(s)	1 (d)	(s)	1 (d)
C(9)	121.00	120.96	120.90	120.90	120.89	120.46	120.50	120.47
$^3J_{CP}$	(s)	7 (d)	7 (d)	8 (d)	(s)	7 (d)	7 (d)	8 (d)
C(10)	133.61	132.05	132.04	132.12	133.73	132.57	132.61	132.74
$^2J_{CP}$	(s)	4 (d)	1 (d)	5 (d)	(s)	4 (d)	5 (d)	5 (d)
C(A)	–	222.1	210.9	199.8	–	222.9	211.9	200.7
$^2J_{CP}$		7 (d)	23 (d)	22 (d)		6 (d)	24 (d)	23 (d)
C(B)	–	217.2	206.2	197.8	–	217.5	206.5	198.3
$^2J_{CP}$		14 (d)	9 (d)	8 (d)		14 (d)	9 (d)	8 (d)

Upon coordination of phosphorus to the metal centre, the J_{CP} coupling constants behaved in a same manner for both phenyls and methoxyphenyls in all complexes: $^1J_{CP}$ coupling constants increased in magnitude, $^2J_{CP}$ coupling constants decreased, $^3J_{CP}$ coupling constants increased and $^4J_{CP}$ coupling constants became observable.

The shielding of the carbonyl carbons increased in the order Cr < Mo < W, together with the increasing number of electrons in the metal [62]. The spectra of the complexes exhibited two carbonyl doublets due to the carbonyls oriented *trans* and *cis* to phosphorus. $^2J_{CP}$ coupling constants of the carbonyl groups followed the same trend as for

the (P,S) donor derivatives: for chromium complexes $|^2J_{CP}(cis)|>|^2J_{CP}(trans)|$ and for molybdenum and tungsten complexes $|^2J_{CP}(cis)|<|^2J_{CP}(trans)|$.

*Table 6. ^{13}C-{^1H} chemical shifts (ppm) and J_{CP} coupling constants (Hz) for (P,O) donor ligands (**L6**,**L7**) and complexes **15-18**). See scheme 4 for numbering of carbon atoms.*

	L6	**15**	**16**	**17**	**L7**	**18**
OCH_3	55.63	54.39	54.51	54.57	55.64(*o*)	55.45(*o*)
					55.07(*p*)	55.20(*p*)
C(1)	–	–	–	–	126.81	123.98
$^1J_{CP}$					7 (d)	41 (d)
C(2)	–	–	–	–	135.61	136.00
$^2J_{CP}$					23 (d)	13 (d)
C(3)	–	–	–	–	113.92	113.82
$^3J_{CP}$					8 (d)	1 (d)
C(4)	–	–	–	–	160.08	160.93
$^4J_{CP}$					(s)	2 (d)
C(5)	124.69	120.73	120.75	120.26	125.72	122.54
$^1J_{CP}$	13 (d)	37 (d)	36 (d)	42 (d)	12 (d)	37 (d)
C(6)	161.52	159.77	159.95	159.92	161.15	159.42
$^2J_{CP}$	17 (d)	4 (d)	5 (d)	4 (d)	16 (d)	7 (d)
C(7)	110.15	110.96	110.95	111.03	110.12	110.75
$^3J_{CP}$	(s)	4 (d)	4 (d)	4 (d)	(s)	4 (d)
C(8)	129.82	131.56	131.50	131.72	129.89	131.65
$^4J_{CP}$	(s)	1 (d)	1 (d)	1 (d)	(s)	1 (d)
C(9)	120.78	119.90	120.01	119.96	120.79	120.39
$^3J_{CP}$	(s)	9 (d)	9 (d)	10 (d)	(s)	7 (d)
C(10)	133.77	134.58	134.70	135.04	133.48	132.39
$^2J_{CP}$	(s)	9 (d)	10 (d)	10 (d)	(s)	4 (d)
C(A)	–	223.4	212.6	201.3	–	223.0
$^2J_{CP}$		6 (d)	24.5 (d)	23 (d)		7 (d)
C(B)	–	217.8	206.7	198.7	–	217.6
$^2J_{CP}$		14 (d)	9 (d)	7 (d)		14 (d)

The ^{31}P-{^1H} NMR data of the complexes are presented in table 7. The ^{31}P chemical shifts increased upon coordination of the ligand to the metal centre. The coordination shifts decreased in the order Cr > Mo >W, in agreement with the observation that decrease of the ^{31}P chemical shift should be observed as one descends in a given periodic group [63]. The chemical shift of the complex decreased with increasing number of *o*-methoxy substituents in the ligand. Coordination shifts, on the other hand, increased with the number of *o*-methoxy substituents. *p*-methoxy substituent reduced the coordination shift (compare complexes **12** and **18**).

*Table 7. ^{31}P-{^{1}H} chemical shifts (δ_P, ppm) and ^{31}P coordination shifts ($\Delta\delta$, ppm) for complexes **8**-**10**, **12**-**18** ($\Delta\delta = \delta_P(complex) - \delta_P(ligand)$).*

L	δ_P	Cr complex	δ_p	$\Delta\delta_P$	Mo complex	δ_p	$\Delta\delta_P$	W complex	δ_p	$\Delta\delta_P$
L4	-16	**8**	53	68	**9**	32	48	**10**	15	31
L5	-27	**12**	48	75	**13**	24	51	**14**	7	33
L6	-38	**15**	42	80	**16**	22	60	**17**	3	41
L7	-28	**18**	43	71	-			-		

Structures of complexes **8**-**14** and **17**-**18** were determined by single crystal X-ray diffraction study and structures of complexes **15** and **16** have been published earlier [66].

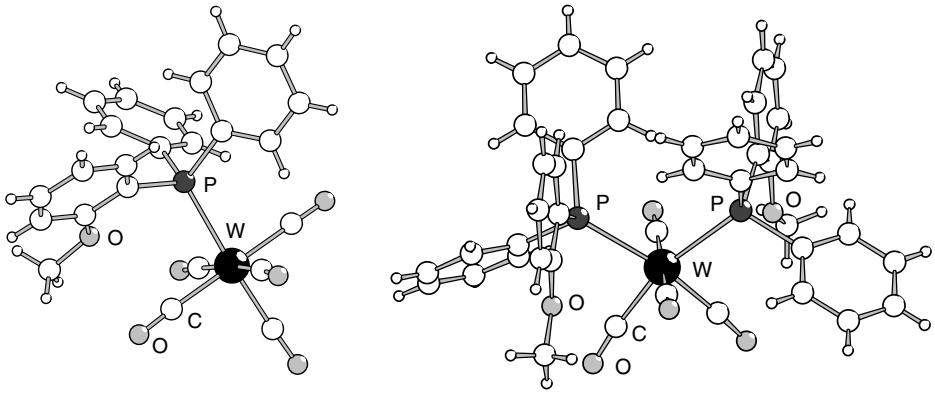

Fig. 3. Crystal structures of monosubstituted complex [W(CO)$_5$(P(*o*-OMePh)Ph$_2$)] (10) and disubstituted complex *cis*-[W(CO)$_4$(P(*o*-OMePh)Ph$_2$)$_2$] (11). Complexes [Cr(CO)$_5$(P(*o*-OMePh)Ph$_2$)] (8) and [Mo(CO)$_5$(P(*o*-OMePh)Ph$_2$)] (9) have structures analogous to 10.

The structures of all the complexes showed slightly distorted octahedral geometry. The phosphane ligand had replaced one carbonyl ligand, except the complex **11** (see fig. 3). Bond lengths behaved in a similar manner as in the complexes of (P,S) donor ligands: chromium hexacarbonyl derivatives had the shortest metal–to–ligand bond lengths, while molybdenum derivatives tended to have slightly longer bonds around the metal centre than the tungsten derivatives. The carbonyl ligand *trans* to phosphane had a slightly shortened M–C bond compared to the *cis* carbonyls, reflecting the relative *trans* influence of the donors (P < CO).

The disubstituted complex *cis*-[W(CO)$_4$(P(*o*-OMePh)Ph$_2$)$_2$] (**11**, see fig. 3) had longer W–P bond lengths (2.566 Å, 2.562 Å) than its monosubstituted analogue **10** (W–P 2.554 Å). This can be explained by the increased steric crowding caused by the two ligands in *cis* positions. W–P bonds of the corresponding complex *trans*-[W(CO)$_4$(P(*o*-OMePh)Ph$_2$)$_2$] [67] are 2.489 Å, shorter than in both **10** and **11**, probably due to relative *trans* influences of the phosphane and carbonyl ligands. All W–C bonds were slightly

shorter in the sterically more crowded complex **11** than in the monosubstituted complex **10**. Complex **11** has a very wide P–M–P angle of 108.4°, in agreement with the long M–P distances due to steric crowding.

An interesting feature of complex **11** is that it crystallised as a *cis* isomer, although, with bulky phosphane ligands, it should favour the *trans* isomer [56]. The crystal structure showed two weak interligand interactions between the methoxyphenyl and phenyl rings of the neighbouring phosphanes, with distances of 3.535 Å and 3.514 Å between the *ortho* CH carbons of the *o*-methoxyphenyl rings and the *ortho* CH carbons of the corresponding phenyl rings. These interactions may favour the *cis* conformer. Anyhow, the complex **11** was a minor product of the synthesis and not very stable in solution.

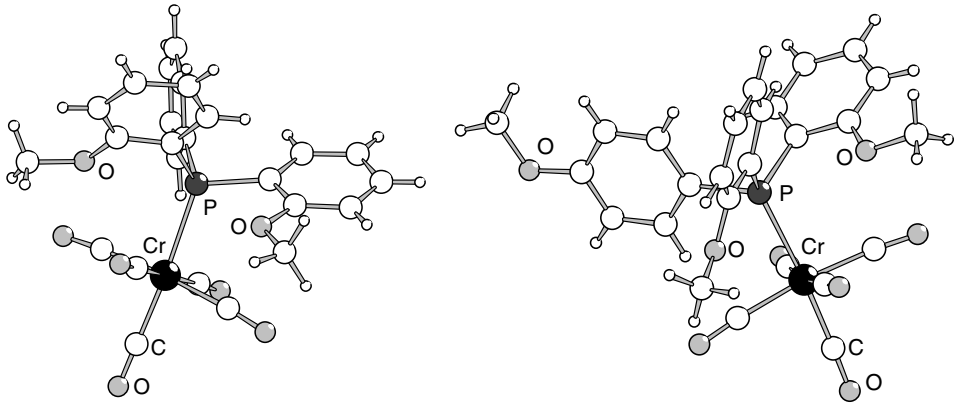

Fig. 4. Crystal structures of sterically similar complexes [Cr(CO)$_5$(P(*o*-OMePh)$_2$Ph)] (12) and [Cr(CO)$_5$(P(*o*-OMePh)$_2$(*p*-OMePh)] (18). Complexes [Mo(CO)$_5$(P(*o*-OMePh)$_2$Ph)] (13) and [W(CO)$_5$(P(*o*-OMePh)$_2$Ph)] (14) have related structure to 12.

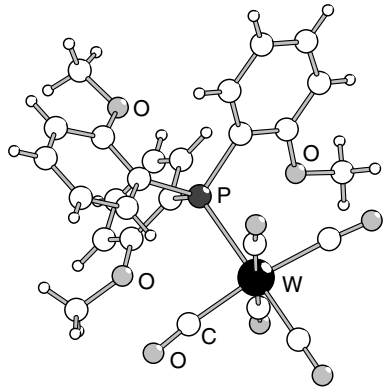

Fig. 5. Crystal structure of [W(CO)$_5$(P(*o*-OMePh)$_3$)] (17). Structures of [Cr(CO)$_5$(P(*o*-OMePh)$_3$)] (15) and [Mo(CO)$_5$(P(*o*-OMePh)$_3$)] (16) are analogous.

3.3.1 Cone angles of methoxy substituted arylphosphanes

The steric crowding of ligands P(*o*-OMePh)Ph_2 (**L4**), P(*o*-OMePh)$_2$Ph (**L5**), P(*o*-OMePh)$_3$ (**L6**) and P(*o*-OMePh)$_2$(*p*-OMePh) (**L7**) was measured using Tolman´s semicone angle method for unsymmetrical phosphanes [6,13]. The cone angles for the free ligands were determined by theoretical calculations with fixed M–P bond distance, and the cone angles for the group 6 complexes were determined from the crystal structure data. All the cone angles were determined at the University of Joensuu [II].

*Table 8. Low lying conformations, the energies related to ground state conformations (ΔE) and the corresponding cone angles (θ) of ligands **L4**-**L6**.*

	L4		**L5**		**L6**	
Conformations	ΔE	θ(°)	ΔE	θ(°)	ΔE	θ(°)
1 (global minimum)	0	166	0	183	0	205
conformation 2	8.9	156	8.7	174	8.1	188
conformation 3	12.6	153	10.6	169	12.1	197
conformation 4			32.9	165	30.5	177
conformation 5					31.4	169
conformation 6					36.5	169

The equilibrium geometries of the free ligands P(*o*-OMePh)Ph_2 (**L4**), P(*o*-OMePh)$_2$Ph (**L5**) and P(*o*-OMePh)$_3$ (**L6**) were determined by optimising the structures by *ab initio* Hartree–Fock method using a 3-21G* basis set. The energies of the minima in relation to ground state (ΔE) are presented in table 8. The number of low lying conformers increased with the degree of substitution of the ligand. As shown in table 8, the cone angles were widest for the ground states and became narrower for the higher energy conformers, so giving an indication of the energy demands of the steric repulsion. A comparison of the calculated cone angles of the free ligands and the structurally determined angles of the complexes is given in table 9.

*Table 9. Cone angle data for free and coordinated ligands **L4**-**L7**.*

L	Free ligand	Free ligand	Flexibility range	Coordinated ligands (X-ray)		
	(X-ray)	(HF-3-21G*)	(HF-3-21G*)	$Cr(CO)_5L$	$Mo(CO)_5L$	$W(CO)_5L$
L4	162	166	153-166	159	158	157
L5	-	183	165-183	173	172	160
L6	-	205	169-205	176	-	172
L7	-	185	-	180	-	-

In the lowest energy conformations, the maximum semicone angles of the ligands are always determined by the *ortho*- or *meta*-hydrogen atoms of the phenyl rings or by one of the hydrogens in an OMe group. For the higher energy conformations, the cone angle

diminishes when the substituted phenyl ring(s) rotate in such a way that the OMe group is located inside the cone and no longer determines the maximum cone angle.

Having only one substituent group, the free ligand P(o-OMePh)Ph_2 (**L4**) did not experience a great deal of either electronic or steric strain from equatorial carbonyl groups and could therefore lie near to its lowest energy conformation in its Cr (**8**), Mo (**9**) and W (**10**) derivatives. Also in the complexes [$Cr(CO)_5$(**L5**)] (**12**) and [$Mo(CO)_5$(**L5**)] (**13**), the ligand P(o-OMePh)$_2$Ph (**L5**) exhibited geometry near to the lowest energy conformations. In the corresponding complex [$W(CO)_5$(**L5**)] (**14**), one of the OMe groups in the substituted phenyl ring lies inside the cone, making the cone angle narrower.

The sterically most crowded ligand, P(o-OMePh)$_3$ (**L6**), seemed to experience considerable strain when coordinated to transition metals, as evidenced by the wide deviation between the calculated low energy cone angles for free ligand and measured cone angles for complexes. Cone angle values of 176° and 172° were observed for Cr derivative **5** and W derivative **17**, respectively. However, the mean CPC angle was larger in both complexes than in the ground state conformation of the free ligand.

3.3.2 Steric and electronic properties of methoxy substituted arylphosphanes and their complexes

Variations in M–P bond distances may depend on both the electronic and steric properties of the ligands. In this study, Cr–P bonds lengthened when the ligand was changed in the order P(*o*-OMePh)Ph_2 (2.387 Å) < P(*o*-OMePh)$_2$(*p*-OMePh) (2.422 Å) ≤ P(*o*-OMePh)$_2$Ph (2.424 Å) < P(*o*-OMePh)$_3$ (2.457 Å). The Mo–P and W–P distances showed similar trends.

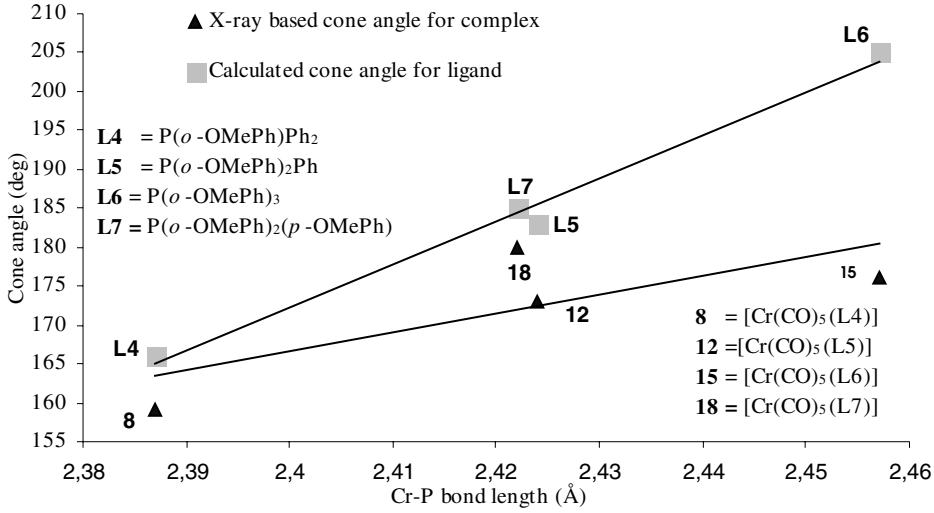

Scheme 5. Cone angle data for free ligands and complexes as a function of Cr–P bond length. Regression correlation r^2=0.988 for ligands and r^2=0.581 for complexes.

Scheme 5 shows the calculated cone angles of the free ligands and the X-ray based cone angles of chromium complexes plotted as a function of Cr–P bond length. Calculated cone angle values for the free ligands correlate well with the observed Cr–P distances (r^2=0.988), but the correlation is not good for the measured cone angles for complexes (r^2=0.581). The reason for this difference is that the steric stress changes the conformations of the ligands in the real complexes. The increasing difference between the calculated and X-ray based cone angles with increase in the steric crowding of the ligands is partly due to the increase in the Cr–P bond length, which influence the X-ray based cone angles. Previous investigations [64,68] support the conclusion that increased steric restrictions of the ligand cause lengthening of the M–P bond.

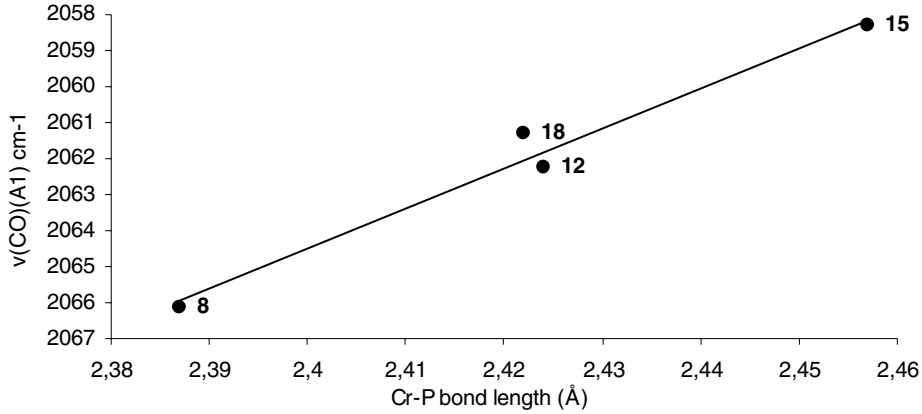

Scheme 6. Basicity of the ligands plotted as a function Cr–P bond lengths. The basicity increases upward in the figure. The values υ(CO) are based on the empirical electron donor–acceptor term defined by Tolman [11]. Regression correlation r^2=0.976.

Small substituents in *para* position can be used to alter solely the electronic properties of the ligand. The cone angle was nevertheless slightly increased with substitution of the *para*-methoxy group (compare ligands **L5** and **L7** or complexes **12** and **18**).

The electronic properties of the ligand affect to the character of the metal–ligand bond [6]. More electronegative substituents on phosphorus are expected to shorten the M–P bond [13]. According to the empirical equation of Tolman [11], the basicities (electron donor properties) of the ligands in this study increase in the order P(*o*-OMePh)Ph_2 < P(*o*-OMePh)$_2$Ph < P(*o*-OMePh)$_2$(*p*-OMePh) < P(*o*-OMePh)$_3$. The Cr–P bond distances of complexes **8**, **12**, **15** and **18** lengthened monotonically with increasing basicity of the ligand (scheme 6). Regression correlation r^2 was 0.976, indicating that the Cr-P bond lengths correlated with basicity as well as with the calculated cone angles of the ligands.

The ^{31}P chemical shifts of complexes of the type [$Cr(CO)_5$L] in which L is halide or aryl substituted phosphane are affected simultaneously by electronegativity, steric properties and the π-bonding capability of the ligand. In complexes in which L is alkyl and aryl substituted phosphane in turn, the ^{31}P chemical shift depends mostly on the steric properties of the ligand [69]. A ^{31}P NMR study of a series of *o*-, *m*- and *p*-substituted

Group 6 arylphosphane complexes indicate that the increasing steric demands of the ligands increase the coordination shift {$\Delta\delta_P=(\delta_P(\text{complex})-\delta_P(\text{free ligand})$} [70].

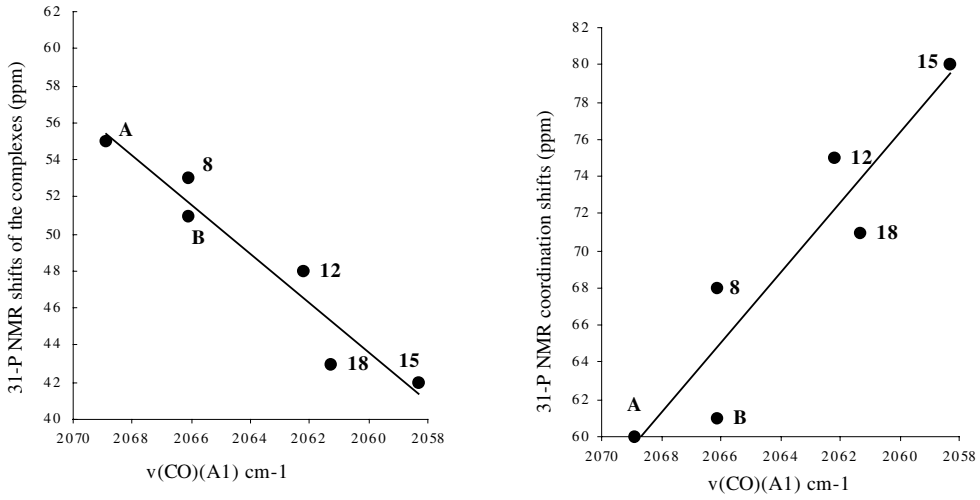

Scheme 7. ^{31}P chemical shifts (left) and ^{31}P coordination shifts (right) of the Cr derivatives plotted as a function of the basicity of the ligand. The basicity increases from left to right. The values υ(CO) are based on the empirical electron donor–acceptor term defined by Tolman [11]. A = [Cr(CO)$_5$PPh$_3$], B =[Cr(CO)$_5$P(*p*-OMePh)$_3$]. Regression correlation: r^2=0.988 (left), r^2=0.865 (right).

A comparison of the ^{31}P NMR data of the chromium carbonyl complexes **8**, **12**, **15**, **18** and [Cr(CO)$_5$P(*p*-OMePh)$_3$] and [Cr(CO)$_5$PPh$_3$] [70,71] revealed that the $\delta(^{31}P)$ of the complexes is probably affected by both the electronic and steric properties of the ligand. The ^{31}P chemical shift correlated well with basicity (r^2=0.988, scheme 7) and reasonably well with both the calculated cone angles of the free ligands (r^2=0.796, scheme 8) and the cone angles determined from X-ray data (r^2=0.865, scheme 8). The ^{31}P coordination shifts showed fairly good correlation with the basicity (r^2=0.865) and calculated cone angles (r^2=0.865) and no correlation at all with the X-ray based cone angles (r^2=0.308). Cr–P bond lengths exhibited better correlation with ^{31}P coordination shifts (r^2=0.901) than with ^{31}P chemical shifts (r^2=0.773).

These results indicate, how difficult it is to draw a line between steric and electronic effects, and between their influences on ^{31}P NMR spectra.

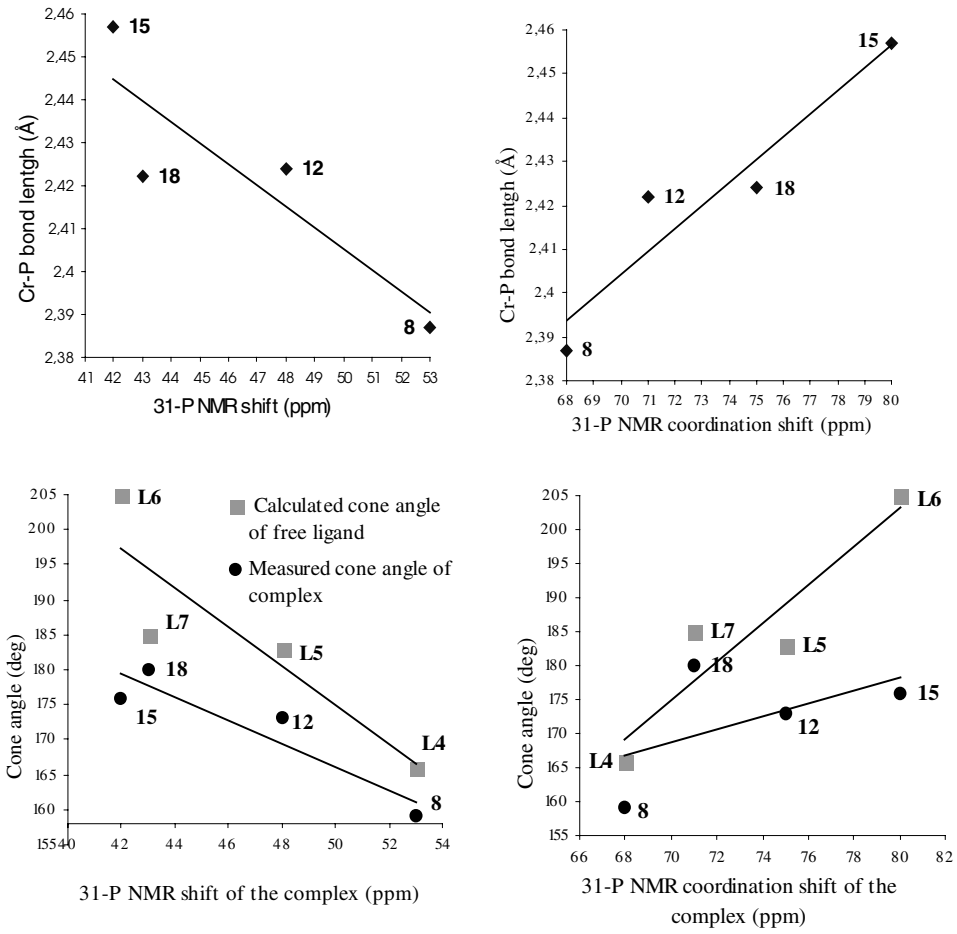

Scheme 8. Cr–P bond lengths (top) and cone angles (bottom) plotted as a function of ^{31}P chemical shifts (left) and ^{31}P coordination shifts (right) of the Cr derivatives. Regression correlations: r^2(top, left)=0.773, r^2(top, right)=0.901, r^2(bottom, left, for free ligands)=0.796, r^2(bottom, left, for complexes)=0.865, r^2(bottom, right, for free ligands)=0.865, r^2(bottom, right, for complexes)=0.308.

4 Disubstituted tungsten carbonyl derivatives of triphenylphosphane and pyridyldiphenylphosphanes

This chapter examines the effect of supramolecular interactions on the *cis/trans* isomerism of $[W(CO)_4L_2]$ type complexes. The aim was to prepare and study complexes in which the phosphane ligands would be cabable of intramolecular attractive interactions. Those interactions could be π-stacking in neutral complexes and cation-π or hydrogen bonding interactions in cationic complexes. 2-Pyridyldiphenylphosphane (P(2-Py)Ph_2), 4-pyridyldiphenylphosphane (P(4-Py)Ph_2) and triphenylphosphane (PPh_3) as shown in scheme 9, were chosen as the ligands. All of these ligands are bulky and sterically closely similar. Scheme 9 shows the complexes (**19**-**25**) that were studied.

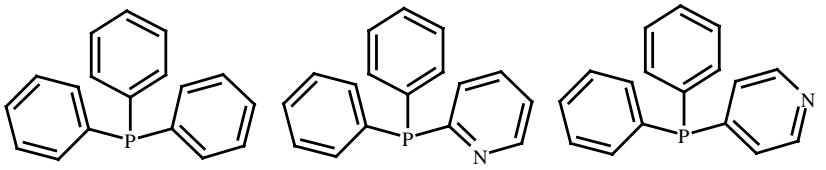

PPh_3 (**L8**) P(2-py)Ph2 (**L9**) P(4-py)Ph2 (**L10**)

19 $[W(CO)_4(\mathbf{L8})_2]$ **21** $[W(CO)_4(\mathbf{L9})_2]$ **25** $[W(CO)_4(\mathbf{L10})]_2$

20 $[W(CO)_4(\mathbf{L8})(py)]$ **22** $[W(CO)_4(\mathbf{L9}\text{-}H^+)(\mathbf{L9})]ClO_4^-$

23 $[W(CO)_4(\mathbf{L8})(\mathbf{L9})]$

24 $[W(CO)_4(\mathbf{L8})(\mathbf{L9}\text{-}H^+)]ClO_4^-$

Scheme 9. Numbering for ligands and their tungsten tetracarbonyl derivatives.

Cis/trans isomerism in complexes of the type $[W(CO)_4(PR_3)_2]$ is normally affected by phosphorus ligand size, the *cis/trans* ratio decreasing as the cone angle of the ligand increases [13,56]. The mechanism of *cis/trans* isomerisation has earlier been studied with the PPh_3 derivative of tungsten [72] and with PR_3 derivatives of molybdenum [73,74,75,76]. *Cis*-$[W(CO)_4(PPh_3)_2]$ is concluded to undergo isomerisation to *trans* isomer via a slow, intramolecular scrambling process [72]. This is in contrast to the analogous molybdenum complex, for which isomerisation takes place via a mechanism

involving Mo–P bond fission [73,74]. Mo complexes with smaller phosphanes undergo isomerisation by a non–bond-breaking mechanism [75]. All these studies consider the interactions between phosphane ligands as repulsive. Even if reaction the route is chosen so as to produce *cis* isomer, subsequent rearrangement to *trans* form will take place. Our study shows that this trend can be reversed by inducing attractive interactions between ligands.

4.1 Reactions

Complexes **19**-**21** and **25** (see scheme 9) were synthesised in an overnight reaction between $[W(CO)_4(Py)_2]$ and phosphane ligand in benzene solution at 40-45°C [56]. The reaction in which PPh_3 was used as ligand, gave a mixture of complexes: $[W(CO)_4(PPh_3)_2]$ (**19**) and $[W(CO)_4(PPh_3)(Py)]$ (**20**). When P(2-Py)Ph_2 and P(4-Py)Ph_2 were used as ligands, the only products that could be isolated from the reactions were complexes $[W(CO)_4(P(2\text{-}Py)Ph_2)_2]$ (**21**) and $[W(CO)_4(P(4\text{-}Py)Ph_2)]_2$ (**25**), respectively. There were no signs of a derivative analogous to **20**. Complex $[W(CO)_4(PPh_3)(P(2\text{-}Py)Ph_2)]$ (**23**) was prepared from **20** by the method described above. In the case of complexes **19**, **21** and **23**, a mixture of *cis* and *trans* isomers was formed. When these complexes were purified by column chromatography, the *cis* isomer was eluted slightly faster than the *trans* isomer but with the bands partially overlapping. *Cis*-$[W(CO)_4(P(2\text{-}Py)Ph_2)_2]$ has been prepared by different method before [77].

Complexes **21** and **23** were protonated with perchloric acid in chloroform solution to give the compounds $[W(CO)_4(P(2\text{-}Py)Ph_2)(P(2\text{-}PyH)Ph_2)^+]ClO_4^-$ (**22**) and $[W(CO)_4(P(2\text{-}PyH)Ph_2)^+(PPh_3)]ClO_4^-$ (**24**). Reaction between $[W(CO)_4(Py)_2]$ and P(4-Py)Ph_2 afforded a structure in which the N atoms of the pyridyl rings of the ligands were attached to the metal centre, forming a bimetallic tungsten tetracarbonyl derivative (complex **25**). No monometallic derivative analogous to **19**, **21** or **23** was formed even when excess of ligand was used, and protonation studies were not pursued.

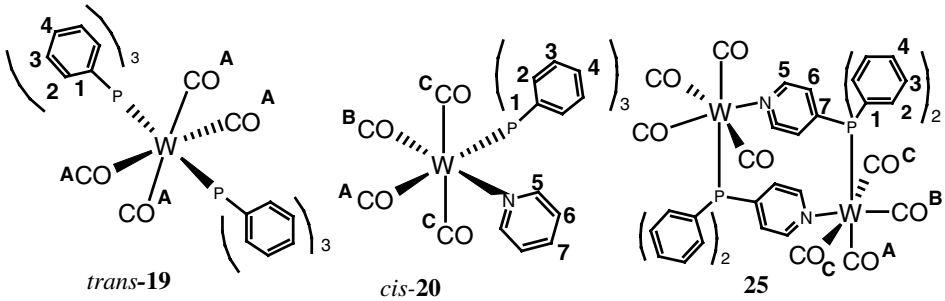

Scheme 10. Numbering of hydrogen and carbon atoms in complexes 19, 20 and 25 (tables 10 and 11).

4.2 Structure and characterisation of complexes

^{1}H NMR and ^{13}C-{^{1}H}NMR data of complexes **19, 20** and **25** and the corresponding free ligands, are presented in tables 10 and 11. Scheme 10 shows the numbering of the H and C atoms of the complexes. The aromatic area of ^{1}H NMR spectra was not of first order and no coupling constants are reported.

*Table 10. ^{1}H chemical shifts (ppm) of complexes **19, 20** and **25** and the corresponding free ligands **L8** (PPh_3), pyridine and **L10** ($P(4\text{-}Py)Ph_2$). See scheme 10 for numbering of hydrogen atoms.*

	L8	**Py**	*trans*-**19**	*cis*-**20**	**L10**	**25**
H(2-4)	7.27-7.33	–	7.26-7.56	7.25-7.41	7.32-7.41	7.48, 7.76
H(5)	–	8.59	–	8.39	8.51	8.23
H(6)	–	7.23	–	6.82	7.11	6.65
H(7)	–	7.62	–	7.49	–	–

*Table 11. ^{13}C-{^{1}H} chemical shifts (ppm) and J_{CP} coupling constants (Hz) of complexes **19, 20** and **25** and the corresponding free ligands **L8** (PPh_3), pyridine and **L10** ($P(4\text{-}Py)Ph_2$). See scheme 10 for numbering of carbon atoms.*

	L8	**Py**	*trans*-**19**	*cis*-**20**	**L10**	**25**
C(1)	137.17	–	137.87	134.33	134.90	132.38
$^{1}J_{CP}$	10 (d)		20 (dd)	37 (d)	10 (d)	41(d)
C(2)	133.70	–	133.09	133.35	134.16	133.93
$^{2}J_{CP}$	19 (d)		6 (dd)	12 (d)	20 (d)	13 (d)
C(3)	128.45	–	128.07	128.32	128.80	129.16
$^{3}J_{CP}$	7 (d)		5 (dd)	9 (d)	8 (d)	10(d)
C(4)	128.66	–	129.34	129.61	129.51	131.25
$^{4}J_{CP}$	(s)		(s)	2 (d)	(s)	(s)
C(5)	–	149.94	–	155.41	149.25	154.40
$^{3}J_{CP}$		(s)		2 (d)	4 (d)	7 (d)
C(6)	–	123.75	–	124.66	127.20	128.89
$^{2}J_{CP}$		(s)		(s)	15 (d)	9 (d)
C(7)	–	135.75	–	135.72	134.90	145.93
$^{1}J_{CP}$		(s)		(s)	10 (d)	22 (d)
C(A)	–	–	203.7	208.7	–	208.5
$^{2}J_{CP}$			6 (t)	37 (d)		(d)
C(B)	–	–	–	210.0	–	203.7
$^{2}J_{CP}$				5(d)		7 (d)
C(C)	–	–	–	204.7	–	198.9
$^{2}J_{CP}$				7(d)		(s)

^{1}H NMR and ^{13}C-{^{1}H}NMR data of complexes **21**-**24** and the corresponding free ligands, are presented in tables 12 and 13. Scheme 11 shows the numbering of the H and C atoms of these complexes. The aromatic area of ^{1}H NMR was of first order here, either.

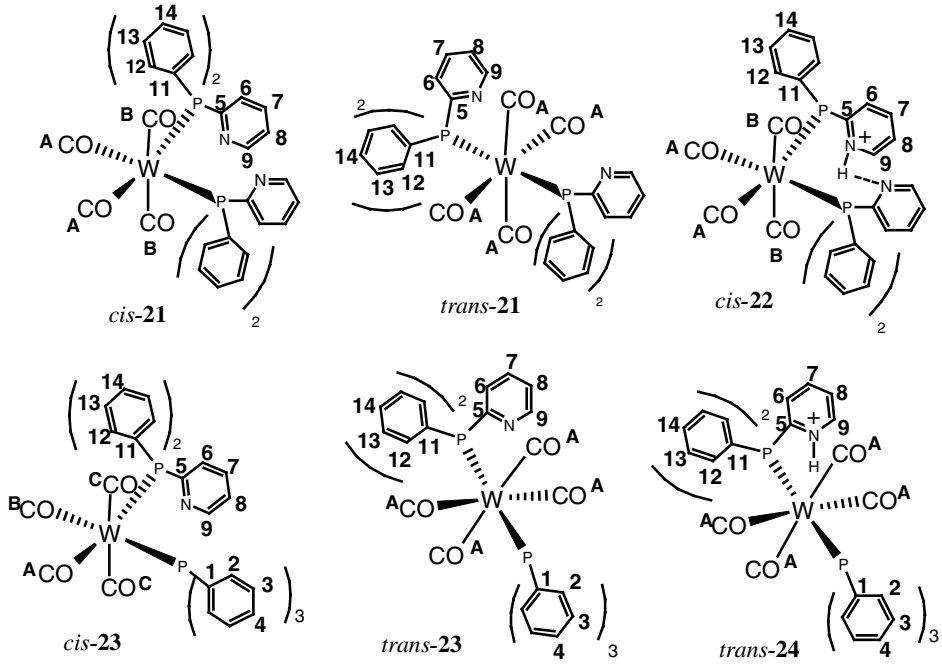

Scheme 11 Numbering of hydrogen and carbon atoms in complexes 21-24 (tables 12 and 13).

*Table 12. ^{1}H NMR chemical shifts (ppm) of complexes **21-24** and the ligand P(2-Py)Ph$_2$ (**L9**). See scheme 11 for numbering of hydrogen atoms.*

	L9	*cis*-**21**	*trans*-**21**	*cis*-**22**	*cis*-**23**	*trans*-**23**	*trans*-**24**
H(2-4)	–	–	–	–	7.20-7.30	7.67, 7.25-7.45	7.20-7.90
H(6)	7.07	7.02	7.29	7.23	6.97	7.29	7.20-7.90
H(7)	7.54	7.41	7.59	7.89	7.45	7.59	7.20-7.90
H(8)	7.16	7.06	7.15	7.38	7.08	7.16	7.20-7.90
H(9)	8.71	8.51	8.78	8.18	8.55	8.80	9.16
H(12)	7.32-7.42	7.45	7.65	7.34	7.59	7.67	7.20-7.90
H(13,14)	7.32-7.42	7.22-7.34	7.32-7.42	7.44-7.51	7.20-7.42	7.25-7.45	7.20-7.90

In the ^{13}C–{^{1}H} NMR spectra of symmetrically substituted complexes *trans*-**19** (table 11) and *cis*-**21**, *trans*-**21** and *cis*-**22** (table 13), phosphane ligands were virtually coupled [78], causing the ^{13}C-^{31}P coupled resonance peaks in aromatic area to appear as triplets in the

spectra (identified as doublets of doublets (dd) in tables 11 and 13). In the case of unsymmetrical complexes, spectra showed normal doublets for $^{13}C–^{31}P$ coupling.

In the case of complexes forming a mixture of *cis* and *trans* isomers, the spectrum of each isomer was measured starting from the pure isomer obtained by column chromatography if possible. In the case of ^{13}C NMR spectroscopy, however, the measurements took so long that the isomer did not remain pure during the measurement. In the case of complex **23** (table 13), the *cis* and *trans* isomers could not be separated from each other and measurements were made initially from their mixture.

*Table 13. ^{13}C-{^{1}H} chemical shifts (ppm) and J_{CP} coupling constants (Hz) of complexes **21-24** and the corresponding free ligands **L8** and **L9.** See scheme 11 for numbering of carbon atoms.*

	L8	**L9**	*cis*-**21**	*trans*-**21**	*cis*-**22**	*cis*-**23**	*trans*-**23**	*trans*-**24**
C(1)	137.17	–	–	–	–	138.00	138.00	136.44
$^{1}J_{CP}$	10 (d)					(d)	40 (d)	43 (d)
C(2)	133.70	–	–	–	–	133.52	133.09	132.99
$^{2}J_{CP}$	19 (d)					11 (d)	12 (d)	11 (d)
C(3)	128.45	–	–	–	–	127.92	128.05	128.44
$^{3}J_{CP}$	7 (d)					9 (d)	9 (d)	10 (d)
C(4)	128.66	–	–	–	–	129.38	129.32	129.7-
$^{4}J_{CP}$	(s)					1 (d)	1 (d)	130.3
C(5)	–	163.91	161.82	162.98	156.29	158-172	158-172	157.85
$^{1}J_{CP}$		4 (d)	(m)	(m)	48(d)			9 (d)
C(6)	–	127.72	127.26	127.24	127.80	127.01	127.27	128.61
$^{2}J_{CP}$		16 (d)	9 (dd)	11 (dd)	4 (d)	18 (d)	22 (d)	6 (d)
C(7)	–	135.62	135.32	135.46	141.02	135.33	135.77	143.96
$^{3}J_{CP}$		3 (d)	(m)	4 (dd)	(s)	6 (d)	12 (d)	(s)
C(8)	–	122.08	122.7	122.78	126.07	122.99	122.87	126.46
$^{4}J_{CP}$		(s)	(s)	(s)	(s)	(s)	(s)	(s)
C(9)	–	150.20	149.31	149.40	147.52	149.31	149.38	145.18
$^{3}J_{CP}$		12 (d)	(m)	7 (dd)	4 (dd)	16 (d)	16 (d)	6 (d)
C(11)	–	136.11	135.93	137.61	134.78	137.47	137.47	134.13
$^{1}J_{CP}$		12 (d)	(m)	21(dd)	22 (d)	(d)	41 (d)	13 (d)
C(12)	–	134.08	133.94	135.53	133.57	133.84	133.52	133.35
$^{2}J_{CP}$		19 (d)	6 (dd)	6 (dd)	6 (dd)	11 (d)	11 (d)	13 (d)
C(13)	–	128.52	127.98	128.02	129.48	127.92	128.07	128.44
$^{3}J_{CP}$		6 (d)	4 (d)	5 (dd)	5 (dd)	9 (d)	9 (d)	10 (d)
C(14)	–	128.95	129.52	129.41	131.47	129.65	129.49	131.4-
$^{4}J_{CP}$		(s)	(s)	(s)	(s)	2 (d)	1 (d)	130.2
C(A)	–	–	203.0	202.95	202.0	intensity	203.0	201.8
$^{2}J_{CP}$			7 (t)	6 (t)	7 (t)	too low	6 (dd)	6 (dd)
C(B)	–	–	205.4	–	203.1	intensity	–	–
$^{2}J_{CP}$			(m)		10 (t)	too low		

The ^{31}P-{^{1}H}NMR spectra of complexes **19**–**25** are presented in table 14. The table also shows the proportion of *cis* isomers in the complexes. The same *cis/trans* ratio was reached regardless of the initially predominant conformation. The proportions were confirmed by repeating the measurement after the solution had been standing for one week. Earlier studies have shown that the bulkier the phosphanes, the more they favour *trans* isomers, and the arylphosphanes show only a very small proportion of the *cis* isomer [56]. Even if the reaction route is chosen to produce the *cis* isomer, subsequent rearrangement to *trans* form will take place [72].

*Table 14. ^{31}P chemical shifts (ppm) for complexes **19-25**, and proportion of cis isomers for complexes **19** and **21-24**.*

	$^{31}P_{cis}$ ($^{1}J_{WP}$/Hz)		$^{31}P_{trans}$ ($^{1}J_{wp}$/Hz)		
	PPh_3	**$PPyPh_2$**	**PPh_3**	**$PPyPh_2$**	*%-cis*
19	23 (229)	-	28 (238)	-	32
20	33 (238)	-	-	-	-
21	-	26 (236)	-	30 (285)	56
22	-	28 (244)	-	34 (288)	100
23	24 (d, $^{2}J_{pp}$ 24)	25 (d, $^{2}J_{pp}$ 24)	29 (269; d, $^{2}J_{pp}$ 58)	30 (270; d, $^{2}J_{pp}$ 58)	41
24	21 (d, $^{2}J_{pp}$ 23)	34 (d, $^{2}J_{pp}$ 23)	24 (275; d, $^{2}J_{pp}$ 61)	38 (297; d, $^{2}J_{pp}$ 61)	14
25	-	35 (240)	-	-	-

In this study, complex $[W(CO)_4(PPh_3)_2]$ (**19**) behaved as expected, forming only 32% of the *cis* isomer in solution. When one or two of the PPh_3 ligands were replaced by P(2-Py)Ph_2 ligand, the proportion of the *cis* isomer increased, even though the steric properties of the ligands did not change. When one of the PPh_3 ligands was replaced by P(2-Py)Ph_2 ligand (complex **23**), the *cis* content increased up to 41%, and when both PPh_3 ligands were replaced by P(2-Py)Ph_2 ligands (complex **21**), the *cis* content increased to 56%. When complex **21** was protonated to give the complex $[W(CO)_4(P(2\text{-}PyH)^{+}Ph_2)(P(2\text{-}Py)Ph_2)](ClO_4^{-})$ (**22**), the equilibrium changed entirely to the *cis* form within a few hours. In protonation reaction of complex **23** to complex $[W(CO)_4(P(2\text{-}PyH)^{+}Ph_2)(PPh3)](ClO_4^{-})$ (**24**), the opposite occurred, and the equilibrium was changed almost entirely to the *trans* form. Protonation reactions could be reversed by adding base to a solution of **22** or **24**, the original *cis/trans* ratio was obtained within a few hours in the case of complex **22** and after one night in the case of complex **24**.

Structures of complexes **19**-**22** and **25** were determined by single crystal X-ray diffraction study. Complex **23** did not crystallise properly, and complex **24** decomposed upon crystallisation.

All the complexes had slightly distorted octahedral geometry, the *cis*-disubstituted derivatives having broadened angle between the ligands: diphosphane derivatives **21** and **22** had angles of 99.7° and 95.7° between the phosphane ligands, respectively, and the sterically less crowded pyridine–triphenylphosphane derivative **20** (fig. 6) had N–W–P angle of 91.6°. In contrast, the corresponding bimetallic complex **25** (see fig. 9) had a narrow N–W–P angle of 88.5°. Bond lengths around the metal centres reflect the relative *trans* influences of the N,P and CO donors.

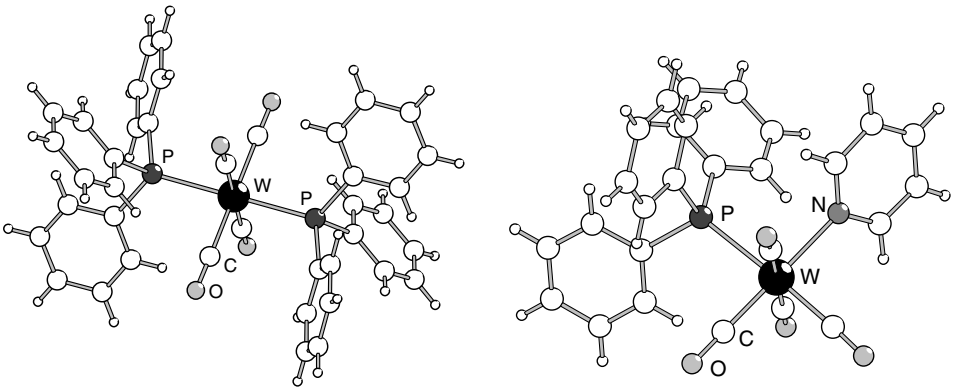

Fig. 6. X-ray structures of complexes *trans*-[W(CO)$_4$(PPh$_3$)$_2$] (19) (left) and cis-[W(CO)$_4$(Py)(PPh$_3$)] (20).

Complex [W(CO)$_4$(PPh$_3$)$_2$] (**19**, fig. 6) crystallised in *trans* form, which is expected for bulky phosphane ligands [56]. Complex [W(CO)$_4$(Py)(PPh$_3$)] (**20**, fig. 6) had a *cis* structure, just as in solution. In the case of complex **20**, there is not much steric stress to make the *trans* form favourable. Surprisingly, complex [W(CO)$_4$(P(2-Py)Ph$_2$)$_2$] (**21**, fig. 7) crystallised in *cis* form, even it is sterically similar to complex **19**. The structure of *cis*-**21** showed face–to–face π-stacking interaction between the pyridyl rings, the centroid–centroid distance of the rings being 3.902 Å. The shortest distance between the atoms of the two rings was 3.527 Å, found between the carbon atoms attached directly to the P atom. The planes were almost parallel, forming an angle of 7.2°. This interaction was intramolecular, not continuous through the crystal lattice.

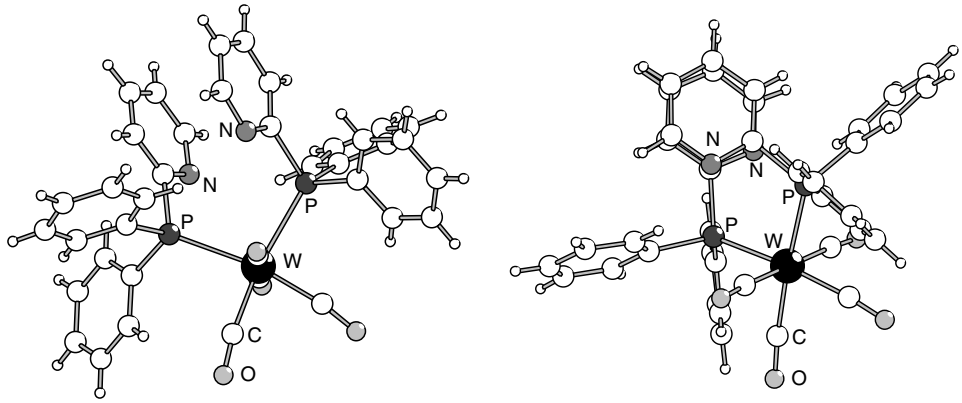

Fig. 7. Structure of complex *cis*-[W(CO)$_4$(P(2-Py)Ph$_2$)$_2$] (21). The view on the right shows the π-stacking of pyridyls.

The protonated derivative of **21**, *cis*-[$W(CO)_4(P(2\text{-}PyH)^+Ph_2)(P(2\text{-}Py)Ph_2)](ClO_4^-)$ (**22**, fig. 8), has a structure in which the N atoms of the pyridyl rings are connected by a hydrogen bond, the distance between the two N atoms being 2.736 Å. Because of the hydrogen bond, the positive charge is shared between the two pyridine rings, and the structure of the complex also shows two cation-π interactions between pyridinium cations and phenyl rings, the centroid–centroid distances of the rings being in one case 3.915 Å, with an angle of 24.0°, and in the other 3.918 Å, with an angle of 19.2°. The shortest distances between the atoms of the rings in both cases is found between the N atoms of the pyridyls and the C atoms attached directly to the P atom in the phenyl rings (3.179 Å and 3.145 Å, respectively).

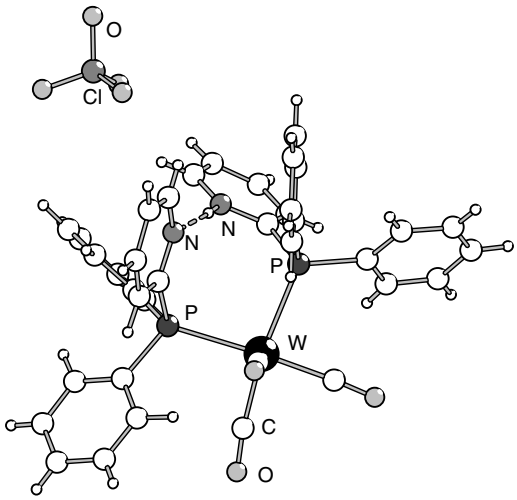

Fig. 8. Structure of the complex *cis*-[$W(CO)_4(P(2\text{-}PyH)^+Ph_2)(P(2\text{-}Py)Ph_2)](ClO_4^-)$ (22).

In addition to π-stacking, other weak interactions may appear in the solid state. Weak hydrogen bonding between the CO ligands and aryl hydrogens was detected in all complexes. This type of interaction has earlier been reported for several transition metal carbonyls [79]. As an example of weak hydrogen bonding, an intermolecular C-O...H distance of 2.53 Å with C-O...H angle of 172.6° is found in complex **19**. Similarly, an intermolecular C-O...H distance of 2.45 with an angle of 161.2° is found in complex **20** and a C-O...H distance of 2.58 Å with C-O...H angle of 162.4° in complex **21**. Complex **22** has two C-O...H distances of 2.52 Å with angles of 157.8° and 161.9°. Since in all these complexes, there are hydrogen bonding interactions that occur between neighbouring molecules, it can be expected that these interactions play no significant role in the *cis/trans* isomerism in solution state.

The X-ray structure of the binuclear complex $[W(CO)_4(P(4\text{-}Py)Ph_2)]_2$ (**25**) is presented in fig. 9. The N–W–P angle is narrow and the carbonyls are pushed away from the phosphane ligand. The pyridyl rings between the tungsten units are parallel, with an angle of 0°, and the distance between the centroids of the rings is 3.286 Å, indicating face–to–face π-stacking interaction. The distance between the centroids is short compared

with the normal attractive π-stacking distance between nitrogen–containing heterocycle planes (between 3.3 and 3.8 Å) [80] and compared with the distance in mononuclear complex *cis*-**21** (3.90 Å). The difference between the π-stacking distances in complexes **21** and **25** may be due to the steric factors present in binuclear complex, or due to the relative difference of the ring polarisation influences of the N atoms of the two structures [81]: in the binuclear structure **25**, the N atoms are at the opposite edges of the aryl rings, while in mononuclear *cis*-**21**, the N-atoms are in adjacent positions (see fig. 7).

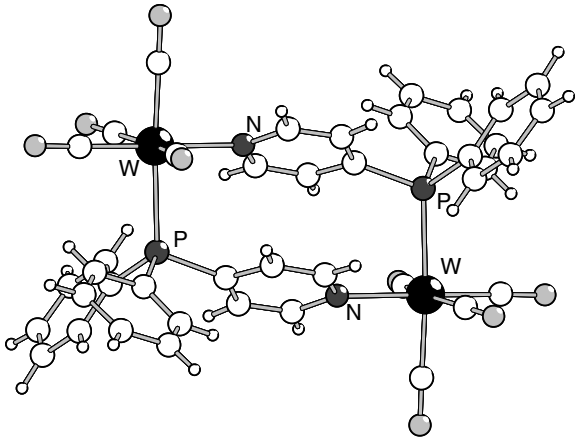

Fig. 9. Structure of complex $[W(CO)_4(P(4\text{-}Py)Ph_2)]_2$ (25).

Complex **25** is the first 4-pyridylphosphane bridged binuclear transition metal complex reported. The only phosphane ligands that have been used as 4-pyridylphosphane type bridges are the diphenylphosphino–terpyridines in trimetallic systems [82,83]. However, Cu(I) and Cd(II) derivatives of bipyridine based ligand that are structurally closely related to $[W(CO)_4(P(4\text{-}Py)Ph2)]_2$ have been reported [84].

4.2.1 Cis/trans isomerisation processes in solution

In solution, attractive and repulsive interactions between ligands have an effect on the isomerisation. Similar interactions occur between the ligands and, for example, solvent molecules, and the net effect of all these, in addition to the electronic properties of the coordination, finally determine the structure. In this work we deliberately varied the attractions between the phosphane ligands in order to change the relative amounts of *cis* isomers.

The differences in solution behaviour of the neutral complexes $[W(CO)_4(PPh_3)_2]$ (**19**), $[W(CO)_4(P(2\text{-}Py)Ph_2)_2]$ (**21**) and $[W(CO)_4(PPh_3)(P(2\text{-}Py)Ph_2)]$ (**23**) (scheme 12) can be

explained in terms of π-π interactions: due to the heteroatom the pyridyl ring is more polarised than the phenyl ring, making the attractive π-π interaction more favourable for the pyridyls than the phenyl rings [81]. In the *cis* isomer with π-π interaction, the steric repulsion between the ligands is minimised and not much attraction is needed between the rings to favour the *cis* form.

In the case of complex **19**, the steric repulsion between the ligands makes the *trans* isomer clearly favoured. There is one pyridyl ring in complex **24**, which could have attractive π-π interaction with one of the phenyl rings, causing the *cis* content to increase slightly relative to complex **19**, but still the *trans* conformation is slightly preferred. In complex **21**, the *cis* conformer is favoured over the *trans* conformer. There the π-stacking between the pyridine rings has been observed by X-ray crystallography (fig. 7).

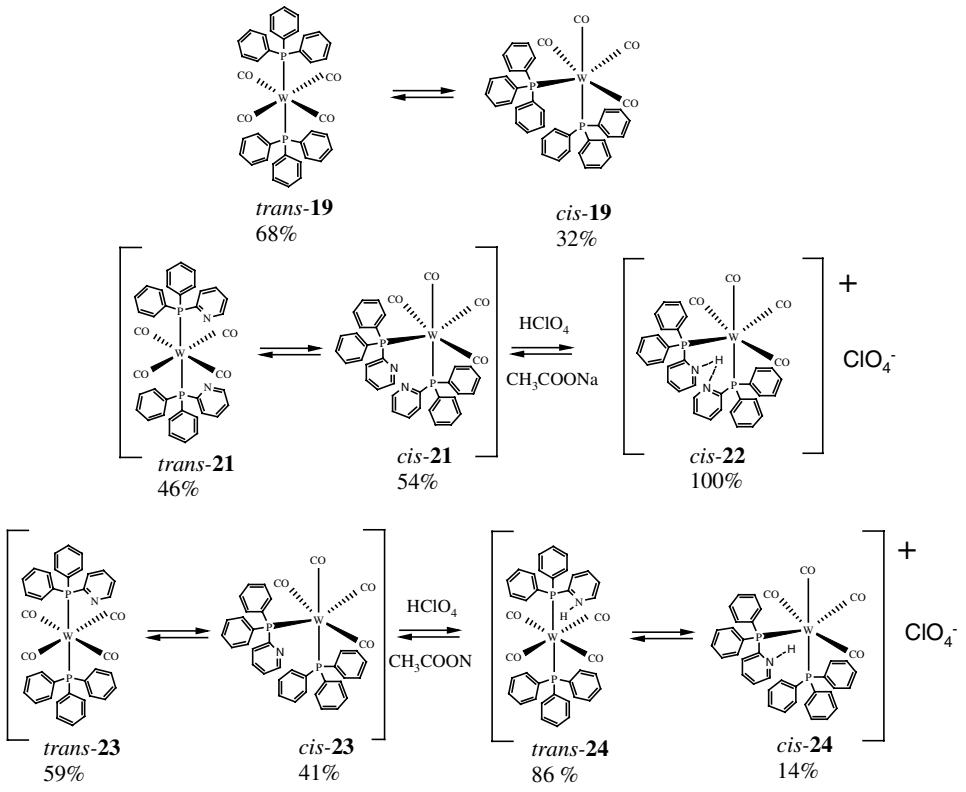

Scheme 12. Solution behaviour of complexes 19 and 21-24. *Cis/trans* ratios were measured by ^{31}P NMR spectroscopy.

The solvent effects are difficult to assess but on grounds of the enthalpies of adduct formation for pyridine (-22 kJ/mol) and benzene (-4.9 kJ/mol) with $CHCl_3$ [85,86], and the empirical solvent polarity parameters of $CHCl_3$ (E_T^N 0.259), pyridine (E_T^N 0.302) and benzene (E_T^N 0.111) [87], pyridine would be expected to exhibit somewhat more

attraction than benzene towards chloroform. The solvent should actually support a higher proportion of *trans* arrangement for complexes **21** and **23** compared to complex **19**, because in the *trans* form the pyridyl groups would maximise their solvent interactions. The structure of **21** (fig. 7) allows fewer possibilities for the solvent attractions of pyridyl groups. With this background, attractive interactions that override both the steric repulsion of bulky ligands and the solvent interactions are needed to explain the observed isomeric ratios.

When complex **21** is protonated, the resulting complex **22** is 100% in the *cis* form (scheme 12). We have isolated the complex $[W(CO)_4(P(2\text{-}PyH)^+Ph_2)(P(2\text{-}Py)Ph_2)](ClO_4^-)$ (**22**) with one protonated pyridyl ring. This structure offers the possibility for an intramolecular N-H...N hydrogen bond (fig. 8). This hydrogen bond, and the two cation-π interactions that were observed, explain the preference for the *cis* isomer.

When complex **23** is protonated, the resulting complex $[W(CO)_4(P(2\text{-}PyH)^+Ph_2)(PPh_3)](ClO_4^-)$ (**24**) is almost totally (86%) in the *trans* form. Now there is only one pyridyl ring to gain the positive charge, and while there is a possibility for intramolecular cation-π bonding between the pyridinium cation and phenyl ring there is no possibility for intramolecular hydrogen bonding. In this case the repulsion between the two phosphane ligands becomes important. Additionally, there is the possibility for intermolecular interactions, such as hydrogen bonding between the pyridinium proton and the ClO_4^- anion, which may also increase the preference for the *trans* isomer. The *trans* form is even more clearly favoured than for the triphenylphosphane derivative **19**. Since the relative strength of the solvent interactions in complexes **22** and **24** should be comparable, the solvent interactions do not explain the structural differences between them.

5 Conclusions

The first part of this work involved study of the coordination of (P,S) and (P,O) heterodonor ligands with Group 6 metal carbonyls. Though the two series of ligands were structurally analogous thiomethoxy and methoxy substituted triphenylphosphane derivatives, their coordination behaviour was different. The (P,S) donor complexes preferred bidentate (P,S) coordination mode, forming five-membered chelates, with the exception of $Cr(CO)_6$, which formed a mixture of monodentate (P) and bidentate complexes with ligand $P(o\text{-}SMePh)_2Ph$. No tri- or tetradentate complexes were formed. The (P,O) donor complexes showed monodentate coordination mode, and appeared to prefer substitution of two phosphane ligands rather than oxygen coordination. The different coordination mode of the two ligand series is consistent with their different behaviour in catalytic hydroformylation [23,25,27,28]. Interest in the ligand chemistry of these *ortho*-SMe and *ortho*-OMe substituted arylphosphanes was aroused by their catalytic potential, which is being studied in our laboratory together with laboratories at the Helsinki University of Technology and the University of Joensuu.

The second part of the work was involved research on attractive interligand interactions between pyridyldiphenylphosphane ligands. Tungsten was chosen as the metal because, findings in the first part of the work showed tungsten to form the most stable complexes.

The steric bulkiness of a ligand and electronic effects like the *trans* influence of a ligand are regarded as major parameters affecting the *cis/trans* isomerism. The most important finding of this study was that the attractive interactions between ligands can be used as a tool to control the relative orientations of the ligands in $W(CO)_6$ derivatives. Protonation reactions could be reversed, which means that the *cis/trans* isomerisation ratio can be tuned with acidity.

Phosphane complexes are used in a variety of catalytic reactions, and the ability to control *cis/trans* isomerism via attractive inter–ligand interactions opens up possibilities for controlling the mechanisms of homogeneous catalytic reactions. The exploitation of similar attractions between ligand and substrate molecules in homogeneously catalysed reactions holds even more promise.

Interestingly, in its structure the complex $[W(CO)_4(P(4\text{-}Py)Ph_2)]_2$ is an organometallic analogue of the [2,2]-paracyclophanes, which are used as building blocks in supramolecular chemistry [88]. Furthermore, the ability of the ligand $P(4\text{-}Py)Ph_2$ to form bridges makes it potential building block for organometallic polymers.

6 References

1. Quin LD (2000) A guide to organophosphorus chemistry, John Wiley & Sons Inc, New York, p. 2, 375.
2. Katti KV, Gali H, Smith CJ, Berning DE (2000) Design and developement of functionalized water-soluble phosphines: catalytic and biomedical implications, Acc Chem Res 32: 9-17.
3. Patai S, Hartely FR (1990) The chemistry of organophosphorus compounds, vol 1, John Wiley & Sons, West Sussex, England, p. 4,192.
4. Henderson WA, Buckler SA (1960) The nucleophility of phosphines. J Am Chem Soc 82: 5794-5800.
5. Henderson WA, Streuli CA (1960) The basicity of phosphines. J Am Chem Soc 82: 5791-5794.
6. Brown TL, Lee KJ (1993) Ligand steric properties. Coord Chem Rev 128: 89-116.
7. Lee KJ, Brown TL (1992) A molecular mechanics model of ligand effects. 2. Binding of phosphines $Cr(CO)_5$. Inorg Chem 31: 289-294.
8. Komiya S (1997) Synthesis of organometallic compounds: A practical guide, John Wiley & Sons, West Sussex, UK, p. 28-34, 125-126.
9. Allmän T, Goel RG (1982) The basicity of phosphines. Can J Chem 60: 716-722.
10. Streuli CA (1960) Determination of basicity of substituted phosphines by nonaqueous titrimetry. Anal Chem 32: 985-987.
11. Tolman CA (1970) Electron donor–acceptor properties of phosphorus ligands. Substituent additivity. J Am Chem Soc 92: 2953-2956.
12. Derencényi TT (1981) Phosphorus-31 nuclear magnetic resonance as a method of predicting ligand basicity and rates of homogeneous catalysis. Inorg Chem 20: 665-670.
13. Tolman A (1977) Steric effects of phosphorus ligand in organometallic chemistry and homogeneous catalysis. Chem Rev 77: 313-348.
14. Abel EW, Stone FGA, Wilkinson G, Labinger JA, Winter MJ (1995) Comprehensive organometallic chemistry II, vol. 5, Vanadium and chromium groups. Pergamon Press, Oxford, p. 239-259.
15. Pignolet L (1983) Homogeneous catalysis with metal phosphine complexes, Plenum Press, New York, p. 257.
16. Cotton FA, Hong B (1992) Polydentate phosphines: their syntheses, structural aspects and selected applications. Prog Inorg Chem 40: 179-289.
17. Bader A, Lindner E (1991) Coordination chemistry and catalysis with hemilabile oxygen–phosphorus ligands. Coord Chem Rev 108: 27-110.
18. Reddy KR, Surekha K, Lee GH, Peng SM, Liu ST (2000) Palladium(II) complexes with phosphorus–nitrogen mixed donors. Efficient catalysts for the Heck reaction. Organometallics 19: 2637-2639.
19. Newkome GR (1993) Pyridylphosphines. Chem Rev 208: 2089-2089.

20. Dilworth JR, Wheatley N (2000) The preparation and coordination chemistry of phosphorus–sulfur donor ligands. Coord Chem Rev 199: 89-158.
21. Dunbar KR, Sun JS, Haefner SC, Matonic JH (1994) Carbon monoxide reactions of the fluxional phosphine complex (η^3-Pr_3)$Mo(CO)_3$ (R=2,4,6-trimethoxyphenyl). Organometallics 13: 2713-2720.
22. Darensbourg DJ, Chojnacki JA, Atnip EV (1993) The catalytic decarbonylation of cyanoacetic acid: anionic tungsten carboxylates as homogeneous catalysts. J Am Chem Soc 115: 4675-4682.
23. Reinius HK, Laitinen RH, Krause AOI, Pursiainen JT (1999) Hydroformylation of methyl methacrylate with heterodonor phosphine rhodium catalysts prepared *in situ*. Catal Lett 60: 65-70.
24. Laitinen RH, Heikkinen V, Haukka M, Koskinen AMP, Pursiainen J (2000) 2-Thioanisyl-dichlorophosphine, new starting material for the preparation of multidentate phosphine ligands: syntheses and characterization of derivatives of 2-anisyl and 2-thioanisyldichlorophosphines. J Organomet Chem 598: 235-242.
25. Reinius HK, Laitinen RH, Krause OAI, Pursiainen JT (2000) Aspects of regioselective control in the hydroformylation of methyl methacrylate with the *in situ* formed (*o*-thiomethylphenyl)-diphenylphosphine rhodium complex. Stud Surf Sci Catal 130A: 551-556.
26. Suomalainen P, Jääskeläinen S, Haukka M, Laitinen RH, Pursiainen J, Pakkanen TA (2000) Structural and theoretical studies of *ortho*-substituted triphenylphosphane ligands and their rhodium(I) complexes. Eur J Inorg Chem 2607-2613.
27. Reinius H, Krause AOI (2000) The effects of process variables in the hydroformylation of methyl methacrylate with the *in situ* formed (o-thiomethylphenyl)diphenylphosphine rhodium complex. J Mol Catal A Chem 158: 499-508.
28. Suomalainen P, Reinius HK, Riihimäki H, Laitinen RH, Jääskeläinen S, Haukka M, Pursiainen J, Pakkanen TA, Krause AOI (2001) Hydroformylation of 1-hexene and propene with in situ formed rhodium phosphine catalysts. J Mol Cat A Chem 3072: 1-12.
29. Laitinen RH, Pursiainen J, Knuutila P, Jääskeläinen S., Koskinen A, Krause O, Pakkanen TA, Reinius H, Suomalainen P (2000) Preparation of heteroarylphosphines as cocatalysts for rhodium catalyzed hydroformylation. PCT Int Appl 39 pp.
30. Steed JW, Atwood JL (2000) Supramolecular chemistry. John Wiley & Sons, England, p. 2, 19-30.
31. Haiduc I, Edelmann FT (1999) Supramolecular organometallic chemistry, Wiley VHC, Germany, p. 95-467.
32. Raymo FM, Stoddart JF (1996) Second-sphere coordination. Chem. Ber. 129: 981-990.
33. Fujita M (1998) Metal-directed self-assembly of two- and three-dimensional synthetic receptors. Chem Soc Rev 27: 417-425.
34. Olenyuk B, Fechtenkötter A, Stang PJ (1998) Molecular architecture of cyclic nanostructure: use of co-ordination chemistry in the building of supermolecules with predefined geometric shapes. J Chem Soc Dalton Trans 1707-1728.
35. Oswald AA, Hendriksen DE, Kastrup RV, Mozeleski EJ (1992) Electronic effects on the synthesis, structure, reactivity and selectivity of rhodium hydroformylation catalysts. Adv Chem Ser 230: 395-418.
36. Oswald AA, Hendriksen DE, Kastrup RV, Irikura K, Mozeleski EJ, Young DA (1987) Steric effects on the synthesis, structure, reactivity and selectivity of rhodium complex hydroformylation catalysts. Phosh Sulfur 30: 237-240.
37. Atkison IM, Lindoy LF (2000) Molecular mechanics and chemical reactivity. A model study of steric effects influencing Co(III) phosphate ester hydrolysis. Coord Chem Rev 200-202: 207-215.
38. Albano BV, Pellon PL, Scatturin V (1966) Zerovalent metal complexes: crystal and molecular structure of [$Pt(PPh_3)_3$]. J Chem Soc Chem Comm 507.
39. Kroener R, Heeg MJ, Deutsch E (1988) Synthesis and charaterization of polypyridine ruthenium(II) complexes containing S-bonded thioether ligands. X-ray crystal structures of *cis*- and *trans*-bis(2,2´-bipyridine)bis(phenothiazine-*S*)ruthenium(II) hexafluorophosphates. Inorg Chem 27: 558-566.

40. Jones GB, Chapman BJ (1997) π Attractive interactions: can they be modulated? Synlett. 439-440.
41. Chapman BJ, Jones GB, Pennington WT (1999) Tricarbonyl (η^6 arene) chromium(0) complex derived from 8-phenylmenthol chiral auxiliary. J Chem Cryst 29: 383-389.
42. Aldrich-Wright JR, Vagg RS, Williams P (1997) Design of chiral picen-based metal complexes for molecular recognition of α-aminoacids and nucleic acids. Coord Chem Rev 166: 361-389.
43. Fanizzi FP, Lanfranchi, Natile G., Tiripicchio A (1994) Platinum(II) complexes with monocoordinated 2,9-dimethyl-1,10-phenantroline and phosphine ligands. Exchange of the donor nitrogen and rotation about the Pt-P and P-C bonds studied by NMR spectroscopy: arene stacking as an intramolecular brake. Inorg Chem 33: 3331-3339.
44. Sorrel T, Epps LA, Kistenmacher TJ, Marzilli LG (1977) Stereoselectivity in the binding of the bis(acetylacenato)(nitro)cobalt(III) moiety to purines and pyrimidines and their nucleosides, an evaluation of the role of interligand interactions in stereoselectivity, and the molecular and crystal structure of the bis(acetylacetonato)(nitro)(deoxyadenosine)cobalt(III) complex. J Am Chem Soc 99: 2173-2179.
45. Szalda DJ, Kistenmacher TJ, Marzilli L (1976) Interligand hydrogen bonding in metal–purine complexes. Crystal and molecular structure of (N-3,4-Benzosalicylidene-N´-methylethylenediamine)(theophyllinato)(aquo)copper(II). Inorg. Chem. 15: 2783-2788.
46. Clot E, Eisenstein O, Crabree RH (2001) How hydrogen bonding affects ligand binding and fluxionality in transition metal complexes: a DFT study on interligand hydrogen bonds involving HF and H_2O. New J Chem 25: 66-72.
47. Hambley TW (1988) Molecular mechanics analysis of the influence of interligand interactions on isomer stabilities and barriers to isomer interconversion in diammine and bis(amine)bis(purine)platinum(II) complexes. Inorg Chem 27: 1073-1077.
48. Jitsukawa K, Iwai K, Masuda H, Ogoshi H, Einaga H (1997) Interligand CH-π interaction in binary cobalt(III) complexes of N-pyridoxy-l-amino acids. Biological significance of the pyridoxal 2-methyl group. J Chem Soc Dalton Trans 3691-3698.
49. Okawa H, Ueda K, Kida S (1982) Noncovalent interactions in metal complexes. 3. Stereo-selectivity caused by interligand, hydrophobic CH-π interaction in 1-l-menthoxy-3-benzoylacetonato complexes. Inorg Chem 21: 1594-1598.
50. Hansen SM, Rominger F, Metz M, Hofman P (1999) The first Grubbs–type methathesis catalyst with *cis* stereochemistry: synthesis of [(η^2-DTBPM)Cl_2Ru=CH-CH=CMe_2] from a novel, coordinatively unsaturated dinuclear ruthenium dihydride. Chem Eur J 5: 557-566.
51. Cornils B, Herrman WA (1996) Applied homogeneous catalysis with organometallic compounds, vol 1, VCH publisher, Weinheim, p. 341-343.
52. Mann FG, Watson J (1948) Conditions of salt formation in polyamines and kindred compounds. Salt formation in the tertiary 2-pyridylamines, phosphines and arsines. J Org Chem 13: 502-531.
53. Meek DW, Dyer G, Workman MO (1976) Bi-, tri-, and tetradentate phosphorus–sulfur ligands, Inorg Synth 16: 168-174.
54. Laitinen RH, Riihimäki H, Haukka M, Jääskeläinen S, Pakkanen TA, Pursiainen J (1999) Syntheses and characterization of new tertiary phosphane ligands prepared from *p*-anisyl and *p*-thioanisyldichlorophosphanes. Eur J Inorg Chem 1253-1258.
55. Shi YL, Gao YC, Shi QZ, Kershner DL, Basolo F (1987) Oxygen atom transfer reactions to metal carbonyls. Kinetics and mechanism of CO substitution reactions of $M(CO)_6$ (M = Cr, Mo, W) in the presence of $(CH_3)_3NO$. Organometallics 6: 1528-1531.
56. Boyles ML, Brown DV, Drake DA, Hostetler CK, Maves CK, Mosbo JA (1985) Relative phosphorus ligand sizes from cis:trans distributions of W(CO)4(L)(L´) products obtained from the reaction of $W(CO)_4$(L)(py) with L´ (L and L´= phosphines), Reaction kinetics, and syntheses of starting materials. Inorg Chem 24: 3126-3131.
57. Kraihanzel CS, Cotton FA (1963) Vibrational spectra and bonding in metal carbonyls. II. Infrared spectra of amine-substituted group VI carbonyls in the CO stretching region. Inorg Chem 2: 533-540.

58. Williams DH, Fleming I (1989) Spectroscopic methods in organic chemistry, 4th edition, McGraw–Hill, London, p. 131-132.
59. Weber L, Wewers D (1985) Übergangsmetallkomplexe instabiler ylide V. Neuartige doppelylide des phosphors als chelatliganden in chromkomplexen. Chem Ber 118: 541-550.
60. Huang Y., Haewon LU, Gilson DFR, Butler IS (1997) Phosphorus-31 chemical shift anisotropies in solid, octahedral chromium(0) triphenylphosphine derivatives. Inorg Chem 36: 435-438.
61. Verkade JG, Quin LD (1987) Methods in stereochemical analysis, vol. 8, Phosphorus-31 NMR spectroscopy in stereochemical Analysis. VCH Publisher Inc, Florida, p. 446.
62. Kunze U, Jawad H (1986) Penta- und tetracarbonylmetall-komplexe des chroms, molybnäns und wolframs mit sekundären und tertiären phosphinothioformamid-liganden. Z Anorg Allg Chem 532: 107-117.
63. Garrou P (1981) Δ_R Ring contributions to ^{31}P NMR parameters of transition metal–phosphorus chelate complexes. Chem Rev 81: 229-266.
64. Aroney MJ, Buys IE, Davies MS, Hambley TW (1994) Crystal structures of $[W(CO)_5(PPh_3)]$, $[M(CO)_5(AsPh_3)]$ and $[M(CO)_5(SbPh_3)]$ (M = Mo, W): a comparative study of structure and bonding in $[M(CO)_5(EPh_3)]$ complexes (E = P, As, Sb; M = Cr, Mo or W). J Chem Soc Dalton Trans 2827-2834.
65. Buchner W, Schenk WA (1984) ^{13}C NMR Spectra of monosubstituted tungsten carbonyl complexes. NMR trans influence in octahedral tungsten(0) compounds. Inorg Chem 23: 132-137.
66. Shawkataly OB, Saminathan T, Muniswaran K, Fun HK, Sivakumar K (1996) Pentacarbonyl-[tris(2-methoxyphenyl)phosphine-P]chromium and its molybdenum analogue. Acta Cryst C52: 1352-1355.
67. Dahlenburg L, Herbst K, Knoch F (1997) Tetracarbonylbis[(2-methoxyphenyl)diphenyl-phosphine-P]tungsten dichloromethane 0.25-Solvate. Acta Cryst C53: 1188-1190.
68. Brown TL (1992) A molecular mechanics model of ligand effects. 3. A new measure of ligand steric effects. Inorg Chem 31: 1286-1294.
69. Vincent E, Verdonck L, Van der Keelen GP (1980) ^{1}H, ^{13}C and ^{31}P NMR studies of some $(C_6H_5)_{3-N}PR_N$ and $(C_6H_5)_{3-N}PR_NCr(CO)_5$ (n = 0–3; R = H, CH_3, C_2H_5, *i*-C_3H_7, *t*-C_4H_9) derivatives. Spectrochim Acta 36A: 699-704.
70. Grim SO, Singer RM, Johnson AW, Randall FJ (1978) A Phosphorus-31 nuclear magnetic resonance study of tertiary phosphine derivatives of group VI metal carbonyls. IV. Substituted triarylphosphines. J Coord Chem 8: 121-126.
71. Bond AM, Carr SW, Colton R, Kelly DP (1983) Comparison of carbon-13 and phosphorus-31 nuclear magnetic resonance data and E° values for a series of chromium pentacarbonyl complexes. Inorg Chem 22: 989-993.
72. Dobson GR, Awad HH, Basson SS (1986) Octahedral metal carbonyls. 61. The mechanism of *cis-trans* isomerisation during ligand-substitution reactions affording *cis*-bis(triphenylphosphine)tetracarbonyl tungsten. Inorg Chimica Acta 118: L5-L6.
73. Darensbourg DJ, Kump RL (1978) A convenient synthesis of *cis*-$Mo(CO)_4L_2$ derivatives (L=group 5A ligand) and a qualitative study of their thermal reactivity toward ligand dissociation. Inorg Chem 17: 2680-2682.
74. Cotton FA, Darensbourg DJ, Klein S, Kolthammer BWS (1982) Steric contributions to the solid–state structures of bis(phosphine) derivatives of molybdenum carbonyl. X-ray structural studies of *cis*-$Mo(CO)_4[PPh_{3-n}Me_n]_2$ (n=0,1,2). Inorg Chem 21: 294-299.
75. Cotton FA, Darensnourg DJ, Klein S, Kolthammer BWS (1982) X-ray structural studies of *cis*-$Mo(CO)_4(PR_3)_2$ (R=Me, Et, *n*-Bu) derivatives and their relationship to solution isomerisation prosesses in these octahedral species. Inorg Chem 21: 2661-2666.
76. Darensbourg DJ, Graves AH (1979) Steric contributions to the solution dynamics involving phosporus ligand dissociation in substituted derivatives of molybdenum hexacarbonyl. Inorg Chem 18: 1257-1261.
77. Zhang ZZ, Wang HK, Shen YJ, Wang HG, Wang RJ (1990) Synthesis of group 6 metal carbonyl complexes containg 2-diphenylphosphinopyridine (Ph_2PPy) and 3,6-

bis(diphenylphosphino)pyrazine (dpppz). The molecular structure of $Cr(CO)_5$(dpppzO) (dpppzO = 3-diphenylphosphino-6-diphenylphospholylpyridazine). J Organomet Chem 381: 45-52.
78. Redfield DA, Nelson JH, Cary LW (1974) Use of "virtually coupled" $^{13}C\{^1H\}$ nuclear magnetic resonance for geometry assignments in bis-phosphine transition metal complexes (1). Inorg. Nucl Chem Lett 10: 727-733.
79. Braga D, Grepioni F (1997) Hydrogen-bonding interactions with the CO ligand in the solid state. Acc Chem Res 30: 81-87.
80. Janiak C (2000) A critical account on π-π stacking in metal complexes with aromatic nitrogen containing ligands. J Chem Soc Dalton Trans 3885-3896.
81. Hunter CA, Sanders JKM (1990) The nature of π-π interactions. J Am Chem Soc 112: 5525-5534.
82. Constable EC, Housecroft CE, Neuburger M, Scheider AG, Springler B, Zehnder M (2000) Programmed assembly of heteromultinuclear complexes using 4´-diphenylphosphino-2,2´:6´,2´´-terpyridine. Inorg Chimica Acta 300-302: 49.
83. Constable EC, Housecroft CE, Catherine E, Scheider G (1999) A clash of cultures: metal carbonyl functionalized Werner complexes. J Organomet Chem 573: 101
84. Hannon MJ, Painting CL, Errington W (1997) Self-assembly of supramolecular boxes. Chem Comm 307-308.
85. Slejko FL, Drago RS (1973) Spectroscopic studies of Lewis acid-base interactions. Nuclear magnetic resonance hydrogen bonding chemical shifts. J Am Chem Soc 95: 6935-6944.
86. Barta L, Kooner ZS, Helpler LG, Roux-Desgranges G, Grolier JPE (1989) Thermodynamics of complex formation in chloroform +1,4-dioxane. Can J Chem 67: 1225-1229.
87. Reichardt C (1994) Solvatochromic dyes as solvent polarity indicators. Chem Rev 94: 2319-2358.
88. Diederich F (1991) Cyclophanes, The Royal Society of Chemistry, Cambridge, p.1-2.